AUGUST 2023

M.Sc in Mechanical Engineering

GHADIR CHAHID

REPUBLIC OF TÜRKİYE

GAZİANTEP UNIVERSITY

GRADUATE SCHOOL OF NATURAL & APPLIED SCIENCES

COMPARISON OF PERFORMANCE PARAMETERS OF A BUILDING HEATING SYSTEM INCLUDING HEAT PUMP AND UNDERGROUND ENERGY STORAGE TANK ASSISTED WITH AND WITHOUT SOLAR ENERGY

M.Sc. THESIS

IN

MECHANICAL ENGINEERING

BY

GHADIR CHAHID

AUGUST 2023

COMPARISON OF PERFORMANCE PARAMETERS OF A BUILDING HEATING SYSTEM INCLUDING HEAT PUMP AND UNDERGROUND ENERGY STORAGE TANK ASSISTED WITH AND WITHOUT SOLAR ENERGY

M.Sc. Thesis

in

Mechanical Engineering

Gaziantep University

Supervisor

Prof. Dr. Recep YUMRUTAŞ

Co-Supervisor

Assist. Prof. Dr. Hatem HASAN ISMAEEL

by

Ghadir CHAHID

August 2023

I hereby declare that all information in this document has been obtained and presented in accordance with academic rules and ethical conduct. I also declare that, as required by these rules and conduct, I have fully cited and referenced all material and results that are not original to this work.

Ghadir CHAHID

ABSTRACT

COMPARISON OF PERFORMANCE PARAMETERS OF A BUILDING HEATING SYSTEM INCLUDING HEAT PUMP AND UNDERGROUND ENERGY STORAGE TANK ASSISTED WITH AND WITHOUT SOLAR ENERGY

CHAHID, Ghadir
M.Sc. in Mechanical Engineering
Supervisor: Prof. Dr. Recep YUMRUTAŞ
Co-Supervisor: Assist. Prof. Dr. Hatem HASAN ISMAEEL

August 2023

72 pages

Underground storage tanks are used to efficiently store thermal energy for domestic and commercial heating systems. This study compares two systems; The first consists of an underground storage tank, a heat pump, and a building to be heated. The second system consists of the same components with adding solar collectors (SC). An analytical model of each system is developed to find the performance parameters of the heating systems. The Coefficient of Performance (COP), the temperature of water in the storage tank, and useful solar energy are part of the main performance parameters. A MATLAB program based on the analytical model is prepared for computing all performance parameters of the heating systems. In the fifth year of operation, the results showed adding the SC led to increasing the temperature of water in the tank by at least 10.2 ℃; it also showed an increase in the value of COP around 1.8. These results were obtained for a tank volume of 400 m^3 , a Carnot efficiency of 40%, and a house in Gaziantep.

Key Words: Energy storage tank, Solar energy, Ground source heat pump, House heating.

ÖZET

ISI POMPASI VE GÜNEŞ ENERJISIYLE VE OLMADAN DESTEKLI YERALTI ENERJI DEPOLAMA TANKI DAHIL BIR BINA ISITMA SISTEMININ PERFORMANS PARAMETRELERININ KARŞILAŞTIRILMASI

CHAHID, Ghadir
Yüksek Lisans Tezi, Makine Mühendisliği
Danışman: Prof. Dr. Recep YUMRUTAŞ
İkinci Danışman: Assist. Prof. Dr. Hatem HASAN ISMAEEL

Ağustos 2023
72 sayfa

Yeraltı depolama tankları, evsel ve ticari ısınma sistemleri için termal enerjiyi verimli bir şekilde depolamak için kullanılır. Bu çalışma, iki sistem arasında karşılaştırma yapar; İlk sistem, yeraltı depolama tankı, ısı pompası ve ısıtılacak bir bina içerir. İkinci sistem, aynı bileşenlere güneş kolektörleri (SC) eklenerek oluşturulur. Her iki sistem için performans parametrelerini bulmak amacıyla analitik bir model geliştirilir. Performans parametrelerinin ana unsurları Performans Katsayısı (COP), depolama tankındaki su sıcaklığı ve kullanışlı güneş enerjisi içerir. Isıtma sistemlerinin tüm performans parametrelerini hesaplamak için bir MATLAB programı hazırlanmıştır. Beş yıl boyunca yapılan işletme sonuçları, SC eklemenin tank içindeki su sıcaklığını en az 10.2 ℃ artırdığını ve COP değerini yaklaşık olarak 1.8 artırdığını gösterdi. Bu sonuçlar, 400 m^3 tank hacmi, Carnot verimliliği 40% ve Gaziantep'teki bir ev için elde edilmiştir.

Anahtar Kelimeler: Enerji depolama tankı, Güneş enerjisi, Yeraltı kaynaklı ısı pompası, Ev ısınması.

"Dedicated to my family"

ACKNOWLEDGEMENTS

I would like to express my deepest gratitude to my supervisor, Prof. Dr. Recep YUMRUTAŞ, and co-supervisor, Assist. Prof. Dr. Hatem HASAN ISMAEEL, for their guidance, support, and invaluable expertise throughout this research. Their mentorship, constructive feedback, and unwavering belief in my abilities have been instrumental in shaping my academic journey.

My heartfelt thanks go to my parents for their love, encouragement, and support. I would like to extend my appreciation to my husband, Radwan, and my children, Delal, Wafa, and Omar. Their unwavering love, understanding, and encouragement have motivated me during this challenging endeavor. Lastly, I am grateful to my brother and sisters for their support.

I am indebted to all those who have contributed to this research in various ways. Your support and belief in me have been invaluable, and I am honored to have you as part of my academic journey.

TABLE OF CONTENTS

LIST OF TABLES

LIST OF FIGURES

Page

LIST OF SYMBOLS

ρ_w	Density of water ($kg.m^{-3}$)
c_w	Specific heat of the water ($kJ.kg^{-1}.K^{-1}$)
V_w	Volume of the water (m^3)
V	Volumeof the tank (m^3)
A	Area of the tank (m^2)
A_c	Area of the solar colletors (m^2)
R	Radius of the tank (m)
r	Radial distance from the tank center (m)
T_w	Water temperature in the tank (K)
T_∞	Eearth temperature (K)
T_i	Inside design air temperature (K)
T_a	Ambient air temperature (K)
T_h	Temperature of the radiator used in the house (K)
K	Thermal conductivity ($W.m^{-1}.K^{-1}$)
α	Thermal Diffusivity ($m^2.s^{-1}$)
Φ_w	Dimensionless water temperature in the tank (-)
Φ_i	Dimensionless inside design air temperature (-)
Φ_a	Dimensionless ambient air temperature (-)
Φ_0	Constant (-)
Q_h	Heat requirement of the house (W)
Q_u	Useful solar energy (W)
Q	Net energy charge to the tank (W)
q_h	Dimensionless heat requirement of the house (-)
q_u	Dimensionless useful solar energy (-)
q	Dimensionless net energy charge to the tank (-)
τ	Dimensionless time (-)
w	Dimensionless heat pump work (-)

γ	Dimensionless parameter (-)
u	Dimensionless parameter (-)
x	Dimensionless radial distance (-)
UA	Product of heat transfer coefficient and area ($W.K^{-1}$)
$(UA)_h$	Product of heat transfer coefficient and area of the house ($W.K^{-1}$)
t	Time (s)
η_c	Carnot efficiency (-)
η_{col}	Efficiency of the solar collectors (-)
ϕ	Latitude angle (radians)
β	Slope angle (radians)
δ	Declination angle (radians)
ω	Hour angle (radians)
ρ	The ground albedo (-)
I_T	Total radiation on a tilted surface ($W.m^{-2}$)
I	Total radiation on a horizontal surface ($W.m^{-2}$)
I_d	Diffuse radiation ($W.m^{-2}$)
I_b	Beam radiation ($W.m^{-2}$)
I_0	Extraterrestrial radiation on a horizontal surface ($W.m^{-2}$)
K_T	Hourly clearness index (-)
G_{sc}	Solar constant ($W.m^{-2}$)

LIST OFABBREVIATIONS

SC	Solar Collectors
COP	Coefficient of Performance
COP_c	Carnot Coefficient of Performance
CE	Carnot Efficiency
TES	Thermal Energy Storage

CHAPTER 1
INTRODUCTION

The utilization of renewable energy resources has become crucial due to the increasing energy demand, depletion of fossil fuel reserves, unpredictable fuel prices, and mounting apprehensions about global warming [1]. The cost of renewable energy technologies has declined significantly in recent years, making it an increasingly cost-effective alternative to fossil fuels.

Renewable energy sources encompass a variety of options, such as solar power, wind energy, hydroelectricity, geothermal heat, bioenergy, and marine energy. These sources are characterized by their sustainable and continuous nature, as they rely on unlimited and perpetually replenished natural resources. In contrast to fossil fuels, which necessitate the extraction and utilization of finite natural reserves, renewable energy sources offer a more environmentally friendly alternative.

Furthermore, the diversification of renewable energy sources plays a significant role in enhancing the energy independence of nations and communities. Rather than heavily relying on the importation of fossil fuels, countries have the capability to generate their own energy through locally available renewable sources. This shift reduces reliance on external sources and contributes to bolstering energy security.

Wind, geothermal, and solar energy are highly practical options among modern renewable energies due to their advanced development, widespread adoption, abundant availability, and ability to provide base-load or distributed electricity [2].

Wind energy involves converting wind power into usable electricity, offering significant potential for sustainable and environmentally friendly energy generation. Geothermal energy, sourced from the Earth's interior, provides a renewable heat source stored in deep hot rocks or hydrothermal reservoirs. Geothermal fluids, such as steam and mineral-laden hot water (brine), are extracted from high-temperature reservoirs through wells for electricity generation and direct uses. The depths of production wells vary depending on the reservoir's characteristics, ranging from 300 meters to over 3000 meters [3]. However, geothermal power faces challenges such as high initial investment, long payback periods, resource assessment complexities, and social acceptance issues. These disadvantages have contributed to the slower growth of geothermal power compared to wind and solar energy [4].

Solar energy has garnered significant attention for its cost-effectiveness and sustainability. Nevertheless, the challenge of matching energy supply with demand remains a critical issue for solar technology. In response to this challenge, the concept of energy storage has been proposed as a solution, with a particular focus on thermal energy storage (TES) dating back to the 1970s [5]. Energy storage can be categorized into short-term and long-term options, where seasonal thermal energy storage (STES) falls under the latter category. STES aims to harness surplus summer heat to meet winter heating requirements effectively.

In this regard, underground storage tanks have emerged as a practical solution to address the complexities of renewable energy heating systems. By accumulating excess thermal energy during periods of abundance and releasing it during high-demand periods like winter, underground storage tanks ensure a consistent and reliable heating supply. This approach outperforms short-term thermal storage systems, which are comparatively less efficient and more unstable [6].

The fundamental principle of thermal energy storage involves capturing, storing, and utilizing heat energy for diverse applications. It enables the conservation of energy by storing excess thermal energy generated during periods of low demand or high efficiency, only to be released when required, thereby reducing overall energy consumption. This concept revolves around storing heat in a medium or substance capable of retaining thermal energy for an extended period. Depending on the specific application and requirements, common storage mediums such as water, molten salts, phase change materials, and compressed air are utilized as solid, liquid, or gas mediums to store and retain thermal energy effectively.

During the charging phase, thermal energy is transferred to the storage medium through various means, such as direct contact, heat exchangers, or absorption processes. This can involve capturing waste heat from industrial processes, solar energy collection, or utilizing excess energy from power generation systems during off-peak periods. The stored heat energy is then held within the storage medium until needed.

Thermal energy can be stored using three different approaches: sensible storage, latent storage, and thermochemical storage[7]:

1.1 Sensible Heat Storage (SHS)

Thermal energy can be efficiently stored through sensible thermal storage, a technique that does not involve any phase change. This method employs materials with high heat capacities, such as water or rocks, to absorb and release heat. When surplus heat is absorbed during the storage process, the material's temperature rises, and it later releases the stored heat when the temperature decreases, making it a valuable and versatile source of thermal energy for various applications.

Dincer et al. [8] conducted an extensive investigation into sensible heat storage (SHS) systems and the methodologies to assess their suitability for solar thermal applications. The study encompassed various aspects, including the availability and selection criteria of SHS systems, economic considerations, evaluation challenges, viability, environmental impacts, feasibility study criteria, and energy-saving alternatives.

Additionally, T. Bauer et al. [9] focused on utilizing Solar Salt, a mixture of sodium nitrate ($NaNO_3$) and potassium nitrate (KNO_3), for sensible thermal energy storage (TES) within a temperature range of 250°C to 550°C. Their research thoroughly explored the thermophysical properties of Solar Salt, including density, heat capacity, thermal diffusivity, and thermal conductivity.

1.2 Latent heat storage (LHS)

One method employed for thermal energy storage involves latent storage, which utilizes the latent heat of a phase-change material (PCM). During this storage process, the PCM undergoes a phase transition, such as solidification or melting, resulting in the absorption or release of a significant amount of heat without any temperature change. These latent storage systems are highly effective in compactly storing large amounts of energy and are commonly used in various applications, including thermal energy storage, heating, and cooling systems.

In a comprehensive study conducted by S. Jegadheeswaran and Sanjay D. Pohekar [10], they thoroughly investigated the implementation of enhancement techniques in different configurations of Latent Heat Thermal Storage (LHTS) systems. Their primary focus was on understanding how these techniques impact the thermal response of the Phase Change Material (PCM), specifically regarding the phase change rate and the amount of latent heat stored or retrieved. Furthermore, they addressed the challenges associated with the mathematical modeling of LHTS systems incorporating these enhancement techniques.

Additionally, Eui Guk Jung and Joon Hong Boo [11] developed an analytical model to predict the transient thermal behavior of a latent thermal energy storage (LTES) system. This model integrated circular fins attached to the heat pipes, with potassium nitrate (KNO_3) chosen as the phase-change material (PCM) due to its specific phase-change temperature. The charging and discharging modes were assumed to involve pure conduction, and the model provided estimates of heat transfer rates and temperature changes for each row of the heat pipe heat exchanger. The simulation accounted for both melting and solidification processes, considering row-by-row heat transfer. The model's accuracy was thoroughly validated by comparing its predictions with experimental findings.

1.3 Thermochemical storage

Thermochemical energy storage involves utilizing chemical reactions to store and release heat energy. Carefully selected chemical reactions allow heat absorption and retention at high temperatures, followed by heat release when the reaction is reversed or triggered by specific conditions. This efficient process enables the storage and retrieval of substantial amounts of heat energy. Thermochemical energy storage systems typically employ materials with high energy density and favorable reaction kinetics, ensuring effective heat absorption and release. Leveraging the principles of thermochemistry, these systems offer a viable solution for long-term, high-capacity thermal energy storage, promoting energy sustainability and minimizing carbon emissions.

In the context of building applications, many thermochemical energy storage devices are designed primarily for space heating purposes rather than cooling. This preference is due to the availability of high-quality thermal energy for heating from solar radiation, a renewable energy source readily captured by solar collectors for further utilization. Additionally, integrating a thermochemical energy storage system with a long-term seasonal TES system can be a practical approach to reduce the carbon footprint, mitigate greenhouse gas emissions, and contribute to overall environmental sustainability [12].

1.4 The aim of the study

This study aims to conduct a comparative analysis of two heating systems' performance over ten years. The first system comprises an underground storage tank, a heat pump, and a building to be heated. In contrast, the second system includes the same components with the addition of solar collectors (SC). To analyze the heat transfer problem within the underground storage tank, the researchers employed the similarity transformation method and Duhamel's Superposition Technique, which resulted in an equation representing the tank's hourly temperature. The study evaluated periodic performance parameters for both systems, such as the tank's temperature and the heat pump's coefficient of performance, and then compared the results obtained over the ten-year timeframe.

The thesis is structured with several chapters dedicated to investigating and analyzing various aspects of the topic. Each chapter focuses on specific components contributing to the overall understanding and findings of the research. A brief overview of the main components covered in each chapter is provided below:

Chapter 1 introduces the significance of renewable energies, providing a brief overview of the main types, and introduces different types of thermal storage for renewable energies.

Chapter 2 emphasizes the importance of heat pumps and their integration with heat storage, discussing previous studies that have explored this integration in different contexts.

Chapter 3 presents a detailed modeling of each component of the two heating systems discussed in this study. Separate equations are developed for each component, allowing for a comprehensive analysis of their behavior and interactions.

Chapter 4 describes the input data used for analysis, specific computation procedures employed to assess the heating systems' performance, and validation procedures to ensure the accuracy and reliability of the findings.

Chapter 5 showcases the results and conducts in-depth discussions. It presents the outcomes of the analysis and modeling of the heating systems, followed by a comprehensive examination and interpretation of these results.

Chapter 6 presents the study's conclusion, summarizing the essential findings and outcomes. It highlights the main contributions and implications of the research, drawing conclusions from the analysis, modeling, and discussions presented in earlier chapters.

CHAPTER 2
LITERATURE REVIEW

Heat pumps serve as highly efficient heating and cooling systems that harness heat from readily available natural sources like outside air, groundwater, or land. They convert this heat into thermal energy, which can be utilized to warm buildings during winter or cool them in the summer. Compared to traditional heating and cooling systems, heat pumps boast impressive energy-saving capabilities, reducing energy consumption by up to 50-60%. Not only do they contribute to significant energy savings, but they also present an eco-friendly alternative by decreasing dependence on fossil fuels and minimizing harmful emissions. Furthermore, heat pumps require minimal maintenance, translating to time and cost savings for users.

Reducing the extensive consumption of fossil fuels is essential for mitigating harmful emissions, as these sources are constrained by depletion, environmental consequences, and economic factors. In response, governments are intensifying their endeavors to encourage energy conservation and the adoption of renewable sources. However, solely relying on these measures cannot fully satisfy the overall energy demand. To bridge the gap between energy supply and demand, heat storage for solar thermal applications plays a crucial role. By implementing heat storage, the efficient utilization of renewable sources is enhanced, resulting in improved energy conservation [5].

Numerous research studies available in the literature delve into the foundational aspects of system design, the modeling and optimization of performance characteristics, and the experimental analysis of pilot-scale methodologies.

Ucar and Inalli [13] conducted a comparison between three different central solar heating systems featuring seasonal storage. They found that the system with a buried storage tank demonstrated the highest thermal performance and economic savings. Insulating the storage tank and utilizing evacuated tube collectors contributed to increased solar fraction and savings compared to non-insulated storage tanks and flat plate collectors with black paint. The study highlighted that the system with an underground storage tank achieved the highest solar fraction and had more significant solar savings compared to the other two storage systems. In addition, insulation on the tank reduced heat loss, resulting in considerable cost savings for the insulated configuration. Based on the research by Dincer and Rosen [14], it has been indicated by two studies that bermed tanks offer greater economic efficiency compared to fully buried tanks, despite potentially having lower performance in minimizing thermal losses. A bermed tank is partially buried and covered with soil from the top down to ground level, with the top portion being insulated. These tanks require less excavation, leading to reduced initial expenses and facilitating convenient maintenance access. H. Huang et al. [15] show that improving the insulation of the top and lateral surfaces of an underground water tank can increase its storage capacity and reduce the required collector area in a seasonal storage system. In a study conducted by Caliskan et al. [16], various types of thermal energy storage (TES) systems, such as Latent, Thermochemical, and Sensible systems, were examined to evaluate their exergetic, energetic, environmental, and sustainability impacts on building applications under diverse environmental temperatures. The results indicated that among the analyzed TES systems, the aquifer TES demonstrated the highest level of sustainability, whereas the latent TES system exhibited the lowest sustainability.

In their study, M.C. Rodríguez-Hidalgo et al. [17] determined that the size of the storage tank plays a critical role in the performance of a solar plant, particularly when the ratio of the tank's volume (V) to the aperture area of the solar collector (A) is below 0.05 m. They further identified that the optimal size for the storage tank is when the ratio V/A equals 0.08m. In their work, R. Yumrutaş et al. [18] developed a model combining analysis and computing for a solar-assisted heat pump system with an underground seasonal cylindrical storage tank. The model utilizes intricate finite Fourier and integral transform techniques to address the transient temperature field problem. The outcomes highlight the system's feasibility as an alternative to fossil fuel-based systems, with peak water temperatures attained towards the end of summer and lower temperatures observed towards the end of winter. Notably, the type of earth and system size exert a considerable influence on the system's performance, with coarse graveled earth yielding the highest storage temperatures.

Chung et al. [19] utilized a TRNSYS simulation program to assess the thermal and economic performance of a Central Solar Heating Plant with Seasonal Storage. The simulation findings indicated that the system had the potential to meet 39% of the total heat energy demand for the greenhouse and office building. Zhang et al. [20] present a model for a space heating and cooling system that incorporates surface water seasonal energy storage. The performance of the system was evaluated by considering factors such as the building's heat load, the vapor compression heat pump cycle, and the seasonal energy storage in a water pond. According to the study, the volume of the water pond and the thickness of the insulating cover are important design factors that have an impact on how well the system works. The suggested approach has been demonstrated to be energy-efficient and can prevent roughly 16% of compressor work throughout the year. Kuang et al. [21] present an investigation of a solar-assisted heat pump system. To mitigate excessive heat loss from the storage tank, the study suggests including an auxiliary energy source at the load point to minimize energy wastage. Additionally, the study recommends employing radiant coils or other low-temperature heating equipment to enhance the thermal efficiency of solar heat pump combination systems. In their study, Wang and Qi [22] examined the performance of underground thermal storage in an (SGCHPS) for residential buildings using a combination of experimentation and simulation. The efficiency of underground thermal storage was found to be significantly influenced by solar radiation intensity and the ratio between the volume of the water tank and the area of the solar collectors. The study recommended maintaining a reasonable balance between the tank volume and collector area, suggesting an optimal range of 20-40 L/m2 for achieving the best performance. Based on total radiation and solar energy absorbed, the effectiveness of underground thermal storage was found to exceed 40% and 70%, respectively. In their study, Qu and Yin [23] introduce an efficient solar cooling and heating system designed for the Intelligent Workplace. The system incorporates a 4 m^3 storage tank and implements constant temperature control. With a north-south (NS) orientation, the system achieves a cooling efficiency of 39% and a heating efficiency of 20%, resulting in annual savings of 100 kW h/m^2 for cooling and 34 kW h/m^2 for heating. Similarly, an east-west (EW) orientation yields 37% cooling efficiency and 29% heating efficiency, leading to annual savings of 74 kW h/m^2 for cooling and 61 kW h/m^2 for heating.

Yumrutas and Ünsal [24] conducted a study focusing on the annual performance analysis of a solar-assisted ground-coupled heat pump system featuring seasonal energy storage within a hemispherical surface tank. To predict the system's behavior and effectiveness, they developed a computational model. The results revealed that the composition of the surrounding soil had a minimal impact on energy fractions but did affect transient temperature and the annual coefficient of performance (COP). However, the benefits of increasing the tank's radius and burial depth were found to be limited. These findings suggest that shallow surface tanks, when properly insulated, are technically feasible for implementing seasonal energy storage.

M. Inalli [25] developed a numerical model for a cylindrical, two-dimensional underground tank. In their review, Y. Zhang et al. [26] examine the recent advancements in utilizing phase change materials (PCMs) for latent heat thermal energy storage (TES) in building applications. The review emphasizes the significance of carefully selecting PCMs with phase change temperatures that closely match the average room temperature, along with appropriate latent heat and thermal conductivity values. The article suggests that PCM walls, floors, and ceilings could effectively reduce peak electricity periods. P. Hoes et al. [27] employ building performance simulation to explore the potential of the innovative hybrid adaptable thermal storage (HATS) concept. The findings indicate that the HATS concept offers the capability to reduce energy demand and minimize underheating/overheating hours when compared to conventional permanent high/low thermal mass concepts. Moreover, the HATS concept demonstrates potential applicability in moderate climates beyond the scope of this study. The Vanhoudt et al. study [28] concentrated on employing a heat pump and an aquifer thermal energy storage system for heating and cooling the ventilation air in a hospital in Belgium during a three-year period. A total of 1280 tons of CO2 were saved throughout the course of the system's three-year operation, or 71% more primary energy savings than a reference installation. J. Kim et al. [29] studied aThermo-hydraulic modeling of an aquifer thermal energy storage (ATES) system to investigate thermal interference. The modeling results revealed that thermal interference is predominantly influenced by factors such as the distance between boreholes, hydraulic conductivity, and pumping/injection rates. The study found that thermal interference can cause a decrease in system performance of up to 22%. E. Mohamed et al. [30] examined a solar-assisted heat pump system with retrofitted collectors, utilizing black paint, for both domestic hot water and space heating purposes in quasi-static conditions. The findings indicated that the system effectively delivered sufficient space heating during winter, achieving an average coefficient of performance (COP) ranging from 3 to 4, along with a solar collector efficiency ranging from 40% to 75%.

Z. Han et al. [31] proposed a solar-assisted transcritical CO2 heat pump system with phase change energy storage (STCHPS-PCES) to address energy waste and air pollution from heating rural buildings. Simulation results show that the system can meet building heating and hot water demands, with a seasonal COP of 2.56. In addition, the system has an energy-saving rate of 43.55% compared to traditional coal-fired heating in rural areas.

A 500 m2 residential building in Shenyang, China, was used as a case study. Shilin Qu et al. has discussed the benefits of using a solar heat-pump heating system with dual-tank latent heat storage (SHPHS-DLHS) [32]. The study proposed using a combination of COP and a new metric called "η" to assess energy efficiency. The results show that SHPHS-DLHS with latent heat storage has better energy performance than a system with sensible heat storage, with a 50% increase in η and a peak COP of 10.03, 3.5 times greater than that of the water-energy storage system. The paper concluded that operational strategy is critical for storing thermal energy.

Tzivanidis et al. [33] conducted a comparative analysis of three heating systems (solar-driven heat pump, air source heat pump, and fan coil heating system with solar collectors) for a well-insulated building located in Athens. The findings revealed that a solar collector area of 25 m^2, combined with a 1 m^3 storage tank, was sufficient to supply the heat pump. Alternatively, a larger system comprising 40 m^2 of solar collectors and a 1.25 m^3 storage tank achieved solar coverage exceeding 70%. Financial evaluation demonstrated that the air-source heat pump represented the most favorable investment option. However, the solar-driven heat pump outperformed in terms of energy efficiency and offered improved thermal comfort conditions. Y. Qiu et al. [34] introduced an innovative solar-assisted heat pump drying system that incorporates a condenser, integrated evaporator, and water storage tank. The system operated in three different modes according to solar radiation intensity levels. Experimental findings demonstrated that the system achieved a coefficient of performance ranging from 3.21 to 3.49, resulting in significant energy savings of

40.53% in terms of energy consumption. In their proposal, T. Kim et al. [35] introduced a hybrid solar collector capable of functioning as a fin-tube exchanger with fans, even in the absence of solar radiation. A simple thermodynamic model was developed to assess the solar-assisted heat pump (SAHP) system, and the implementation of the SAHP system incorporating hybrid solar collectors demonstrated remarkable performance, operating for 7036 hours per year. The system demonstrated feasibility as an independent solution for hot water supply due to its capability to extend the yearly operation duration, its straightforward configuration, and its economic viability with reduced capital expenses.

In their research article, M. Pinamonti and P. Baggio [36] investigated the utilization of energy storage technologies in solar-assisted heat pump (SAHP) systems to reduce energy demand and installation costs, while improving the self-consumption of solar energy. The study encompassed heating and cooling applications in three buildings with different energy performance levels. The findings indicated that in highly insulated buildings, the combination of photovoltaic (PV) panels and battery storage achieved the highest energy reduction of 30%. For medium-insulated buildings, PV installation was identified as the most cost-effective solution, resulting in a 25% decrease in energy consumption. In contrast, for low-insulated buildings, the integration of solar thermal (ST) panels emerged as the most profitable option, leading to a 26% reduction in energy usage. Additionally, the study identified key factors influencing the performance of SAHP systems. In their work, P. Wu et al. [37] introduced a heating system that incorporates an air source heat pump (ASHP) along with a water storage tank to enhance its efficiency in low ambient temperatures. The system operates on a unique strategy of charging the tank during the day and discharging it at night, resulting in notable energy savings. Monitoring data revealed that the system achieved an average performance coefficient of 2.35 on the coldest day, while the seasonal COP reached 2.95. These values were 14.0% and 26.1% higher, respectively, compared to the continuous operation mode. Additionally, J. Wu et al. [38] experimented with a cascade air-source heat pump water heater that used thermal storage made of phase change material. The heating COP values in the cascade mode ranged from 1.74 to 2.55, whereas the single-stage mode's values ranged from 1.5 to 3.05. Moreover, the water tank equipped with PCM achieved an efficiency of

97.85%, supplying an additional 407 kJ of energy compared to the tank without PCM, which had an efficiency of 94.23%.

Ioan Sarbu and Calin Sebarchievici [39] conducted a comprehensive study on various aspects of Ground Source Heat Pump (GSHP) technology. Their research covered topics such as the utilization of Ground Water Heat Pumps (GWHPs) and their limitations, the introduction of the "Geotherm" system as a potential solution, thorough reviews of heat transfer simulation models and ground thermal response tests for vertical Ground Heat Exchangers (GHEs), discussions on hybrid Ground Coupled Heat Pump (GCHP) systems, and an analysis of the energy, economic, and environmental performance of a hybrid closed-loop GCHP system. The study emphasized the importance of considering heat pump systems during the design process and highlighted the challenges and opportunities involved in replacing traditional heating systems with GSHPs in existing buildings.

Sharma et al. [40] focused on thermal energy storage technology utilizing phase change materials (PCMs) in various applications, including solar water-heating systems, space heating and cooling, and off-peak electricity storage. It highlights the advantages of PCMs, such as high-energy storage density and isothermal storage process, and discusses their wide temperature range suitability for different applications. Finally, the paper provides an overview of current research, assessing the thermal properties of PCMs and melt fraction studies, emphasizing their potential in energy conservation and diverse storage systems.

Hepbasli and Akdemir [41] presented an energy and exergy analysis of a ground source heat pump (GSHP) system applied to a 65 m2 room. The study evaluates the performance and efficiency of the system components using exergy balance equations, providing quantitative insights into inefficiencies and the impact of component modifications. The results highlight areas of high exergy destruction and demonstrate system components' interconnectedness in performance optimization. In a study conducted by Esen et al. [42], performance experiments and economic analysis were carried out on a horizontal ground source heat pump (GSHP) system located in Elazığ, Turkey. The GSHP system demonstrated favorable performance, achieving average coefficient of performance (COP) values of 2.68 and 2.82 for the two heat exchangers, as well as average COP values of 3.13 and 3.42 for the heat pumps. From an economic standpoint, the GSHP system offered advantages over heating methods involving electric resistance, fuel oil, liquid petroleum gas, coal, and oil. However, it was not competitive with natural gas due to the region's relatively low natural gas costs.

A. Amini et al. [43] studied the use of Phase Change Material (PCM) in a Thermal Energy Storage (TES) system to store and release industrial wasted heat. By incorporating finned water-charged heat pipes into the PCM bulk, the low conductivity issue of PCMs was addressed. The experimental results demonstrate the feasibility of using PCM as a thermal storage medium and recovering wasted heat through a heat pipe-based TES heat exchanger. Z. Li et al. [44] comprehensively reviewed latent thermal energy storage (LTES) technology, focusing on medium-high temperature phase change materials for heat recovery, storage, and utilization. Their review covered various aspects, including the thermophysical properties of different PCMs, thermal conductivity enhancement techniques, heat transfer enhancement methods, and applications in different heat recovery systems.

M. Joybari et al. [45] compared the performance of single-tube (SHTX) and multiple-tube (MTHX) shell-and-tube heat exchangers for thermal energy storage using phase change materials (PCMs). The MTHX, which had five HTF tubes, exhibited shorter process times due to a larger heat transfer surface area and more intense natural convection during the melting process. However, increasing the HTF flow rate did not significantly enhance performance, indicating that other heat transfer enhancement techniques are necessary within the PCM.

A polymeric composite for thermal energy storage, utilizing phase change materials (PCMs) with low melt temperature paraffin, was developed by S. Peng et al. [46]. The paraffin was encapsulated within epoxy matrices to form the composite material. The researchers conducted measurements on several properties of the composites, including particle size distribution, thermal conductivity, contact resistance, thermal diffusivity, and latent heat. The results revealed that when the PCM transitioned to a liquid state, the thermal conductivity of the composites increased due to improved wetting of the epoxy by the liquid paraffin. Furthermore, the volume expansion of the paraffin liquid within the composite contributed to the enhanced conductivity. The study examined different epoxy systems as well as a thermoplastic SEBS/paraffin system with varying glass transition temperatures. The findings demonstrated that the interaction between the paraffin and epoxy components yielded satisfactory thermal and mechanical performance in the paraffin/epoxy composite.

In their overview, D. Lefebvre and F.H. Tezel [47] discuss the potential of thermal energy storage through adsorption. While still in the early stages of development, adsorption processes show promise. Successful adsorbents such as zeolite 13X, activated alumina hybrids, silica gel, and alkaline-treated activated alumina have been identified. However, challenges related to adsorbent instability and system variability must be addressed.

Thermal storage has also been used in drying systems where excess heat can be stored and used during periods of low heat availability. This ensures a stable and controlled heat source for the drying process. This approach optimizes energy use, allows better integration of intermittent heat sources, and enhances process control in drying systems. Using Phase Change Materials (PCMs) as a thermal storage medium, large amounts of heat can be stored and released during its transition, providing a reliable and regulated heat source for drying processes. Integrating thermal storage into drying systems improves energy efficiency, reduces energy consumption, and optimizes drying processes.

H. Atalay et al. [48] developed a solar air heater for drying apple slices, and a packed bed thermal energy storage system was designed to ensure continuous drying. In addition, a recuperator unit was utilized for waste heat recovery, allowing the reutilization of 50-60% of waste heat in the drying process. The system demonstrated a significant energy consumption reduction of 76.8% compared to other drying technologies. Experimental tests were conducted twice a day, and the drying kinetics of apple slices at constant temperatures were determined.

H. Hasan Ismaeel and R. Yumrutaş [49] investigated a wheat drying system that utilizes solar energy storage in an underground TES tank. The study shows that the system works periodically after the fifth year, with performance parameters gradually increasing over time. In addition, the surrounding geological structure's thermophysical properties affect the system's functioning.

In a study conducted by E. Baniasadi et al. [50], the performance of a forced convection mixed-mode solar dryer with thermal energy storage was analyzed. The results of the study showed enhanced performance of the solar collector and the ability to extend the drying process practically when solar energy is not available. Additionally, it was observed that the drying rate remained relatively consistent across the drying chamber. The moisture pick-up efficiency of the dryer was approximately 10%, while the overall thermal efficiency reached around 11%.

G. Srinivasan et al. [51] focused on integrating sensible and latent heat storage units in solar dryers. It highlighted the advantages of using heat storage materials such as rocks, pebbles, sand, bricks, water, and paraffin wax for continuous drying and temperature control. Desiccant materials were also explored for sensible heat generation. The review emphasized the need for further research on heat transfer enhancement techniques, such as nano materials, and integrating heat pumps, auxiliary heaters, and solar collectors to ensure continuous operation in all weather conditions.

D. Jain and P. Tewari [52] developed a state-of-the-art solar crop dryer with thermal energy storage to ensure the continuous drying of herbs. The solar crop dryer offers an alternative to traditional open sun drying and effectively utilizes solar radiation for drying. It extended the drying period by maintaining temperatures between 40 and 45°C, and the thermal efficiency of the dryer was found to be 28.2%. With reasonable cost and product prices, the solar dryer proved to be financially viable with a payback period of 1.5 years.

H. Hasan Ismaeel and R. Yumrutaş [53] investigated the thermal performance of a drying system with thermal energy storage (TES) tank and heat recovery unit (HRU). The results indicated that the TES tank volume and collector area depend on the wheat's mass flow rate and moisture content. The COP, COPs, SMER, and TES tank water temperatures are influenced by the wheat's moisture content and solar collector area. Including the HRU reduces energy consumption, and the geological structure around the TES tank affects system performance. The drying system operates periodically after the fifth year, and the system COPs are slightly lower than the heat pump COP.

CHAPTER 3
MODELING OF THE SYSTEM

Air heat pumps are essential components of modern building heating systems, and understanding their behavior is crucial for optimizing energy efficiency and sustainability. These systems operate by transferring heat from a hot source to a cold source using a thermal compressor and a cooling medium. While they work effectively in areas with moderate temperatures, their performance can vary significantly based on various factors.

In the context of this thesis, we delve into the modeling aspect of building heating systems, specifically those that incorporate heat pumps and underground energy storage tanks, both with and without the addition of solar energy. This thesis will study two systems, as depicted in Figure (3.1) and Figure (3.2), providing a comprehensive analysis of their efficiency and effectiveness in meeting heating and cooling requirements.

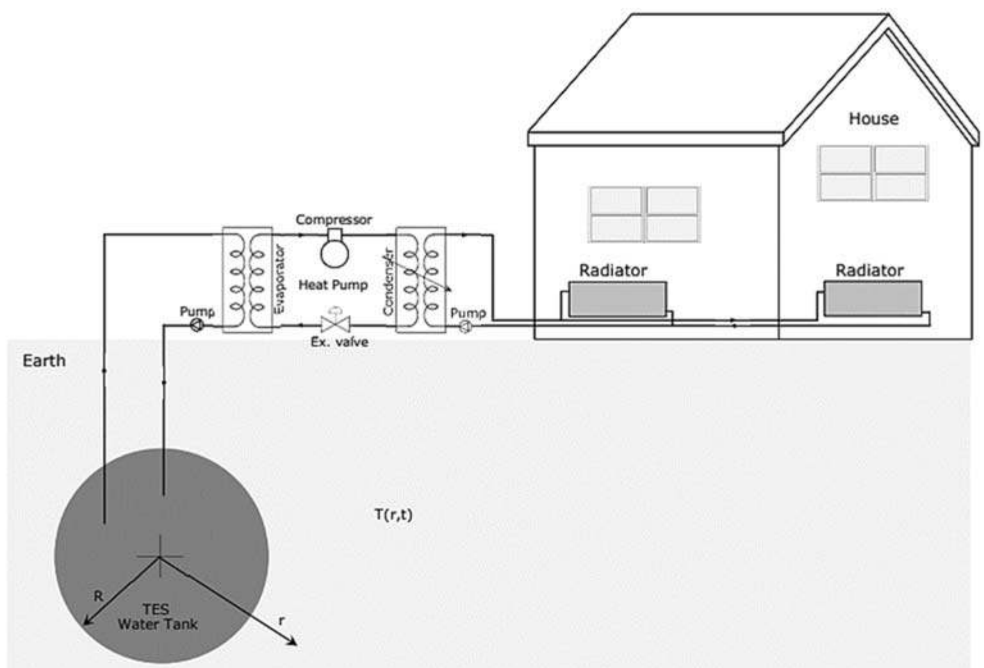

Figure 3.1. Heating system with ground-coupled heat pump.

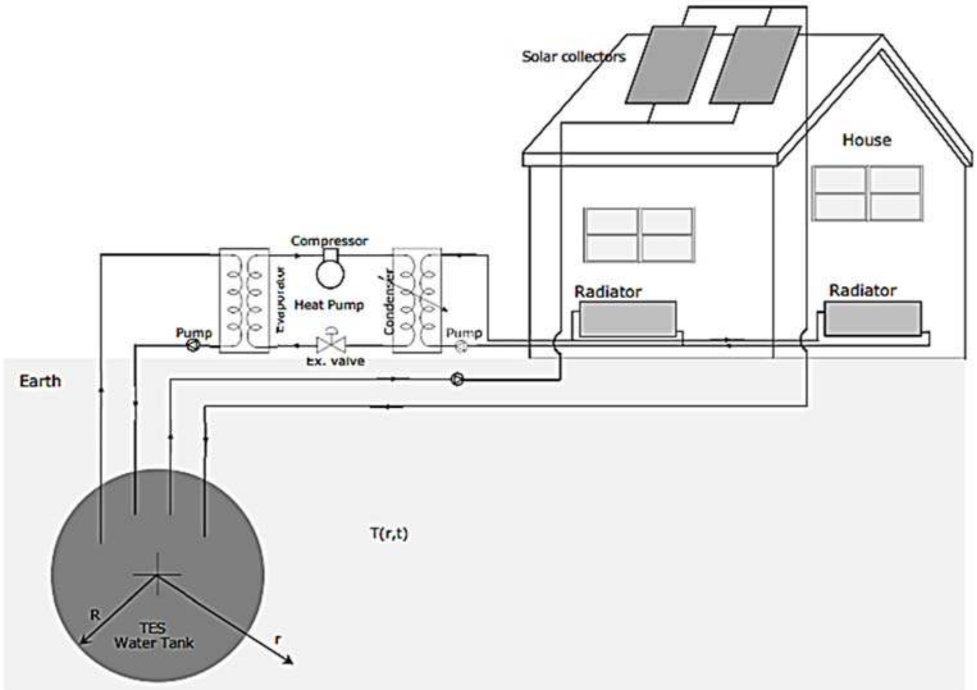

Figure 3.2. Heating system with solar assisted and ground coupled heat pump.

3.1 Modeling of the heating system connected to an underground TES tank only

3.1.1 Solution of the transient heat transfer problem for the TES tank

In this study, it is assumed that the thermal energy storage (TES) tank has a spherical shape and is filled with water. Initially, the water temperature is considered to be equal to the deep underground temperature, denoted as T_∞ . Since the TES tank is located significantly deep below the ground surface, the complex three-dimensional transient heat transfer problem is simplified into a one-dimensional transient heat transfer problem. This simplification enables the analysis of the problem as a one-dimensional unsteady heat transfer problem in spherical coordinates. The temperature of the ground far away from the storage tank is assumed to be constant and equal to T_∞ , allowing for simplification of the analysis. It is assumed that the surrounding Earth's surface has a uniform structure and consistent thermophysical properties.

This section aims to develop an equation for calculating the water temperature inside the TES tank as a function of time, as well as determining the net heat extraction from the TES tank. The initial and boundary conditions of the transient temperature field problem outside the spherical TES tank within the Earth are expressed in spherical coordinates as follows:

$$\frac{\partial^2 T}{\partial r^2} + \frac{2}{r}\frac{\partial T}{\partial r} = \frac{1}{\alpha}\frac{\partial T}{\partial t} \tag{3.1}$$

$$T(R, t) = T_w(t) \tag{3.2}$$

$$T(\infty, t) = T_\infty \tag{3.3}$$

$$T(r, 0) = T_\infty \tag{3.4}$$

By using following dimensionless radial distance (x) , time(τ) and temperature ($\emptyset$) we can obtain the dimensionless form of Eq. (3.1):

$$x = \frac{r}{R} \tag{3.5}$$

$$\phi = \frac{T - T_\infty}{T_\infty} \tag{3.6}$$

$$\phi_w = \frac{T_w - T_\infty}{T_\infty} \tag{3.7}$$

$$\phi_a = \frac{T_a - T_\infty}{T_\infty} \tag{3.8}$$

$$\tau = \frac{\alpha t}{R^2} \tag{3.9}$$

$$\frac{\partial^2 \phi}{\partial x^2} + \frac{2}{x}\frac{\partial \phi}{\partial x} = \frac{\partial \phi}{\partial \tau} \tag{3.10}$$

Boundary conditions are :

$$\phi(1, \tau) = \phi_w(\tau) \tag{3.11}$$

$$\phi(\infty, \tau) = 0 \tag{3.12}$$

$$\phi(x, 0) = 0 \tag{3.13}$$

The energy balance for the storage tank is defined as:

$$Q = \rho_w c_w V_w \frac{dT_w}{dt} - kA\frac{\partial T}{\partial r}(R, t) \tag{3.14}$$

Using dimensionless parameters in Eq. (3.5-3.9) gives:

$$Q = \alpha.\rho.c(4\pi R)\, T_\infty[\frac{\rho_w c_w}{3\rho.c}\frac{d\phi_w}{d\tau} - \frac{\partial \phi}{\partial x}(1, \tau)] \tag{3.15}$$

, where ($k = \alpha.\rho.c$) represents conductivity of the ground ,V_w and A are the volume and area of the TES tank.

$$q = p\frac{d\phi_w}{d\tau} - \frac{\partial \phi}{\partial x}(1, \tau) \tag{3.16}$$

$$\frac{\partial \phi}{\partial x}(1, \tau) = p\frac{d\phi_w}{d\tau} - q \tag{3.17}$$

, where ; $q = Q/k(4\pi R)T_\infty$ and $p = \rho_w c_w/3\rho.c$.

Eq. (3.10) can be further simplified by applying the following transformation:

$$\psi(x, \tau) = x.\phi(x, \tau) \tag{3.18}$$

$$\frac{\partial^2 \psi}{\partial x^2} = \frac{\partial \psi}{\partial \tau} \tag{3.19}$$

$$\psi(1, \tau) = \phi_w(\tau) \tag{3.20}$$

$$\psi(\infty, \tau) = 0 \tag{3.21}$$

$$\psi(x, 0) = 0 \tag{3.22}$$

Using Eq.(3.18) in Eq.(3.17) gives:

$$q = p\frac{d\phi_w}{d\tau} - \frac{\partial \psi}{\partial x}(1, \tau) + \psi(1, \tau) \tag{3.23}$$

The following similarity transformation is used to solve this dimensionless transient heat transfer problem:

$$\eta = \frac{x-1}{2\sqrt{\tau}} \tag{3.24}$$

The solution for the constant ϕ_0 is:

$$\psi(x,\tau) = \phi_0 \left\{1 - \mathrm{Erf}\left[\frac{x-1}{2\sqrt{\tau}}\right]\right\} \tag{3.25}$$

The general solution is obtaind as:

$$\psi(x,\tau) = \phi_w(0)\left\{1 - \mathrm{Erf}\left[\frac{x-1}{2\sqrt{\tau}}\right]\right\} + \int_0^{\tau} \left\{\frac{d\phi_w(\xi)}{d\xi}\right\}\left\{\frac{x-1}{2\sqrt{\tau-\xi}}\right\} \tag{3.26}$$

The following integro-differential equation can be obtained by differentiating the general solution with respect to dimensionless variable x, evaluating the result at x=1, and substituting it into (3.23):

$$q = p\frac{d\phi_w}{d\tau} + \phi_w(\tau) + \int_0^{\tau} \left\{\frac{d\phi_w(\xi)}{d\xi}\right\}\left\{\frac{d\xi}{\pi\sqrt{\tau-\xi}}\right\} \tag{3.27}$$

The finite difference form of Eq.(3.27) is given as follows:

$$\phi_w(\tau_n) = \frac{q(\tau_n) + \left[\frac{p}{\Delta\tau} + \frac{1}{\sqrt{\pi\Delta\tau}}\right]\phi_w(\tau_{n-1}) - \sum_{i=1}^{n-2} \frac{\phi_w(\tau_{n+1}) - \phi_w(\tau_i)}{\sqrt{\pi\Delta\tau(n-i)}}}{1 + \frac{p}{\Delta\tau} + \frac{1}{\sqrt{\pi\Delta\tau}}} \tag{3.28}$$

The dimensionless water temperature in the TES tank can be determined using Eq. (3.28).

The q(τ) term in Eq. (3.28) is equal to the difference between heat pump work and the heat requirement of the house, which can be given as:

$$q(\tau) = \frac{w(\tau)}{\gamma} - q_h(\tau) \tag{3.29}$$

, where $w(\tau)$ and $q_h(\tau)$ represent the dimensionless heat pump work and heat requirement of the house during heating season. ($\gamma = (4\pi R)k/(UA)_h$)is a dimensionless parameter.

3.1.2 Energy requirement of the house

Energy needs of the house in heating season can be expressed as:

$$Q_h(t) = (UA)_h[T_i - T_a(t)] \tag{3.30}$$

, where $(UA)_h$ represents the product of heat transfer coefficient and house's area, T_i represents the inside design air temperature, $T_a(t)$ represents the hourly ambient air temperature.

The energy requirment of the house can also be expressed as:

$$Q_h(t) = (UA)_{he}[T_h(t) - T_i] \tag{3.31}$$

, where $(UA)_{he}$ represents the product of the load side heat exchanger's area employed in the home and heat transfer coefficient, T_h the temperature of the load side heat exchanger utilized within the house.

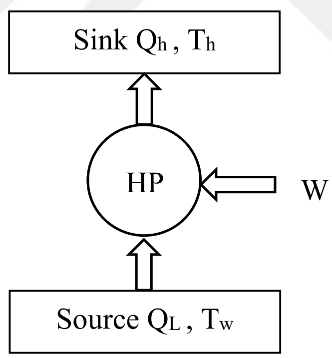

Figure 3.3. Heat pump

3.1.3 Energy requirement of the heat pump

The heat loss in the condenser can be expressed as:

$$Q_h(t) = W(t). COP \tag{3.32}$$

$$W(t) = \frac{Q_h(t)}{COP} \tag{3.33}$$

$$\mathrm{COP} = \frac{\mathrm{Q_h(t)}}{\mathrm{W(t)}} = \frac{\mathrm{Q_h(t)}}{\mathrm{Q_h(t) - Q_L(t)}} \tag{3.34}$$

, where COP represents the coefficient of performance of the heat pump for space heating. COP can be also given as:

$$\mathrm{COP} = \eta_c . \mathrm{COP_c} \tag{3.35}$$

, where η_c is known as a ratio of actual COP of a pump to Carnot COP.

Carnot COP at any time is given as a function of source temperature T_a and sink temperature T_h:

$$\mathrm{COP_c} = \frac{\mathrm{T_h(t)}}{\mathrm{T_h(t) - T_a(t)}} \tag{3.36}$$

$$\mathrm{COP} = \eta_c . \frac{\mathrm{T_h(t)}}{\mathrm{T_h(t) - T_a(t)}} \tag{3.37}$$

Using (u) parameter:

$$\mathrm{u} = \frac{\mathrm{(UA)_h}}{\mathrm{(UA)_{he}}} = \frac{\mathrm{T_h(t) - T_i}}{\mathrm{T_i - T_a(t)}} \tag{3.38}$$

Eq. (37) becomes:

$$COP = \eta c.\ uTi - Tat + Ti[uTi - Tat + Ti] - Tat \tag{3.39}$$

To find the work of the heat pump, we can rewrite Eq. (3.33) using dimensionless forms of the temperatures, which are given as:

$$\phi_a(\tau) = \frac{\mathrm{T_a(t) - T_\infty}}{\mathrm{T_\infty}} \tag{3.40}$$

$$\phi_i = \frac{\mathrm{T_i - T_\infty}}{\mathrm{T_\infty}} \tag{3.41}$$

$$\phi_w(\tau) = \frac{\mathrm{T_w(t) - T_\infty}}{\mathrm{T_\infty}} \tag{3.42}$$

$$Q_h(t) = (UA)_h T_\infty[\phi_i - \phi_a(\tau)] \tag{3.43}$$

Combining Eq. (3.33) and Eq. (3.43) gives:

$$W(t) = (UA)_h T_\infty[\phi_i - \phi_a(\tau)].\frac{\{u[\phi_i - \phi_a(\tau)] + \phi_i - \phi_a(\tau)\}}{\eta_c\{u[\phi_i - \phi_a(\tau)] + \phi_i + 1\}} \tag{3.44}$$

The dimensionless form of the heat pump work $w(\tau)$ is defined as :

$$w(\tau) = \frac{W(t)}{(UA)_h T_\infty} \tag{3.45}$$

$$w(\tau) = \frac{[\phi_i - \phi_a(\tau)].\{u[\phi_i - \phi_a(\tau)] + \phi_i - \phi_a(\tau)\}}{\eta_c\{u[\phi_i - \phi_a(\tau)] + \phi_i + 1\}} \tag{3.46}$$

3.2 Modeling of the heating system connected to an underground TES tank with using solar collectors

For modeling the underground TES tank, heat pump, and the building to be heated, the same equations as in the previous section are followed, with the addition of solar collectors modeling in this section, so the net heat extract from the TES tank is changed.

3.2.1 Solar energy collection rate

The hourly useful energy collection rate $Q_u(t)$ can be calculated by:

$$Q_u(t) = \eta_{col}(t).I_T(t) \tag{3.46}$$

$I_T(t)$ is the hourly radiation on the tilted solar collector which is given by:

$$I_T(t) = R.I(t) \tag{3.47}$$

, where R is the ratio of total radiation on the tilted surface to that on a horizontal surface. It can be estimated by:

$$R = \left(1 - \frac{I_b(t)}{I(t)}\right)R_b + \frac{I_d(t)}{I(t)}\left(\frac{1 + \cos\beta}{2}\right) + \rho\left(\frac{1 - \cos\beta}{2}\right) \tag{3.48}$$

, where β represents the slope angle of the surface ($\beta = 37.1^{\circ}$), ρ represents the ground albedo which is usually taken 0.2 when there is no snow and 0.7 when there is a fresh snow cover [54].

R_b represents the ratio of beam radiation on a tilted surface to the radiation on a horizontal surface, which is given as:

$$R_b = \frac{\cos(\emptyset + \beta) . \cos\delta . \cos\omega + \sin(\emptyset + \beta) . \sin\delta}{\cos\emptyset . \cos\delta . \cos\omega + \sin\emptyset . \sin\delta} \tag{3.49}$$

, where ϕ represents the latitude angle ($\phi = 37^{\circ}$) , ω represents the hour angle (15°per hour of local noon), and δ is the declination angle, it is calculated by:

$$\delta = 23.45 \sin\left(360 \frac{284 + n}{365}\right) \tag{3.50}$$

$\frac{I_d(t)}{I(t)}$ is the ratio of diffuse radiation to total radiation on horizontal surface. It is given by [55]:

$$\frac{I_d(t)}{I(t)} = \begin{cases} 1.0 - 0.249K_T & \text{for } K_T \leq 0 \\ 01.557 - 1.84K_T & \text{for } 0.35 < K_T \leq 0.75 \\ 0.177 & \text{for } K_T > 0.75 \end{cases} \tag{3.51}$$

, where K_T represents the hourly clearness index, and is calculated by:

$$K_T = \frac{I(t)}{I_o(t)} \tag{3.52}$$

$I_o(t)$ represents the extraterrestrial radiation on a horizontal surface for an hour period and is given as:

$$I_o(t) = \frac{12 \times 3600}{\pi} G_{sc} \left(1 + 0.33 \cos\frac{360\, n}{365}\right) \times \left[\cos\phi \cos\delta\, (\sin\omega_2 - \sin\omega_1) + \frac{\pi(\omega_2 - \omega_1)}{180} \sin\phi \sin\delta\right] \tag{3.53}$$

, where G_{sc} represents the solar constant ($G_{sc} = 1353\ w/m^2$), $I(t)$ represents the hourly solar radiation on a horizontal surface which is taken from measurements.

After finding K_T and then $\frac{I_d(t)}{I(t)}$ we can find $\frac{I_b(t)}{I(t)}$ [56]:

$$I_b(t) = I - I_d(t) \tag{3.54}$$

$$\frac{I_b(t)}{I(t)} = 1 - \frac{I_d(t)}{I(t)} \tag{3.55}$$

After finding those values, it can be substituted into Eq.(3.48) to find the value of R and then find the hourly solar radiation on the tilted surface $I_T(t)$, Eq.(3.47).

The efficiency of the flat plate solar collector $\eta_{col}(t)$ in Eq. (3.46) is estimated [56]:

$$\eta_{col}(t) = 0.72 - 6.4\,\frac{T_w(t) - T_a(t)}{I_T(t)} \tag{3.56}$$

, where $T_w(t)$ represents the inlet fluid temperature which is equal to the storage tank temperature. ($T_w(0) = 15$ °C) and $T_a(t)$ represents the ambient air temperature.

Finally, we can calculate $Q_u(t)$the useful solar energy by Eq.(3.46).

Dimensionless form of the useful solar energy is expressed as:

$$q_u = \frac{Q_u}{k(4\pi R)T_\infty} \tag{3.57}$$

By adding the solar collectors SC, the dimensionless net heat input rate to the TES tank in Eq. (3.29) becomes:

$$q(\tau) = q_u(\tau) + \frac{w(\tau)}{\gamma} - q_h(\tau) \tag{3.58}$$

Which will be used in Eq. (3.28) in order to calculate the hourly water temperature in the TES tank.

3.3 Input Data

The system information sources have been validated through scientific references and certified meteorological data. These data were compiled into databases, inputted using their respective identifiers, and subsequently analyzed, ensuring accuracy and the absence of any anomalies. The information was then incorporated into the MATLAB program for analysis and application.

3.3.1 Heat pump parameters and house heating load

CE values ranging from 0.30 to 0.50 for small electric heat pumps were reported by Zogou and Stamatelos [57]. As a result, the present study took into account three CE values (0.30, 0.40, and 0.50) in accordance with their findings. The overall heat transfer coefficient, is considered to be 345W/°C and designed heating load of the house is considered 10 kW. The value of (u) mentioned in Eq. (3.38) was considered equal to 1.2. The inside design temperature is set at 20°C, while the outside design temperature is -9°C.

3.3.2 Thermal storage tank

In this study, the tank volume was assumed to be 400 m^3, with an initial water temperature equal to the ground temperature, $T_w(0) = 15°C$. A density of 1000 kg/m^3 and a specific heat of 4.18 kJ/kg.°C were assigned to the water. The soil surrounding the tank was assumed to be granite, and its physical properties are listed in Table 3.

3.3.3 Solar collectors

The purpose of connecting the system to the solar collectors is to compare its parameters with the other system. The solar collectors are directly connected to the storage tank, with an area of 20 m^2 and a slope angle of $\beta = 37.1°$, which is equivalent to the angle of latitude. The solar constant is 1353 W/m^2. Hourly outside temperatures and solar radiation were obtained from the Meteorological Authority in Gaziantep.

Table 3. Thermophysical characteristics of geological formations as described by Ozisik [58].

Ground Type	Conductivity (W/m K)	Diffusivity ($\times 10^{-7}$) m2 /s	Specific Heat J/kg K	Heat Capacity kJ/m³ K
Coarse	0.519	1.39	1842	3772
Limestone	1.3	5.75	900	2250
Granite	3.0	14.00	820	2164.8

CHAPTER 4
VALIDATION AND COMPUTATION PROCEDURE

4.1 Computation Procedure

In the first heating system which is connected to the underground TES tank without solar collectors (SC), the heat requirement for the house is calculated using Eq. (3.43) along with the pump work through Eq.(3.46) and depending on the initial tank temperature (T_w (0) = 15°C). Next, the dimensionless net heat input to the tank is calculated using Eq. (3.29). The dimensionless water temperature in the TES tank is calculated using Eq. (3.28), and finally, the coefficient of performance COP is calculated over ten years to evaluate and analyze the annual periodic operating condition.

In the second heating system, when solar collectors (SC) are added, the net heat input to the tank is calculated using a different equation (3.58), and the same process is repeated to obtain the required system parameters.

The heat pump operates when the ambient temperature is lower than the inside design temperature in the house.

Figure 4.1 displays the flowchart of the process in MATLAB code used in the system connected to an underground TES tank without using solar collectors (SC). Additionally, Figure 4.2 represents the flowchart of the process in MATLAB code used in the second heating system, which incorporates heat pump, connected to an underground TES tank with solar collectors (SC).

4.2 Validation Procedures

The validation phase in research plays an important role in thoroughly examining the accuracy and reliability of findings. In this section, the process of validation is undertaken to confirm the strength and precision of the modeling and analysis.

In this validation section, a thorough comparison of figures and results from the present study and the previous ones conducted independently, yet yielding remarkably similar outcomes, is carried out.

This section establishes the credibility and significance of the research and the formulas used. It focuses on the validation procedure of the study, involving a comparison between the figures obtained from this study and those we got from previous studies. The equations were applied in the MATLAB program and compared with the results of previous studies, which were applied in the Fortran 90 program, and a match was obtained in the diagrams for both systems.

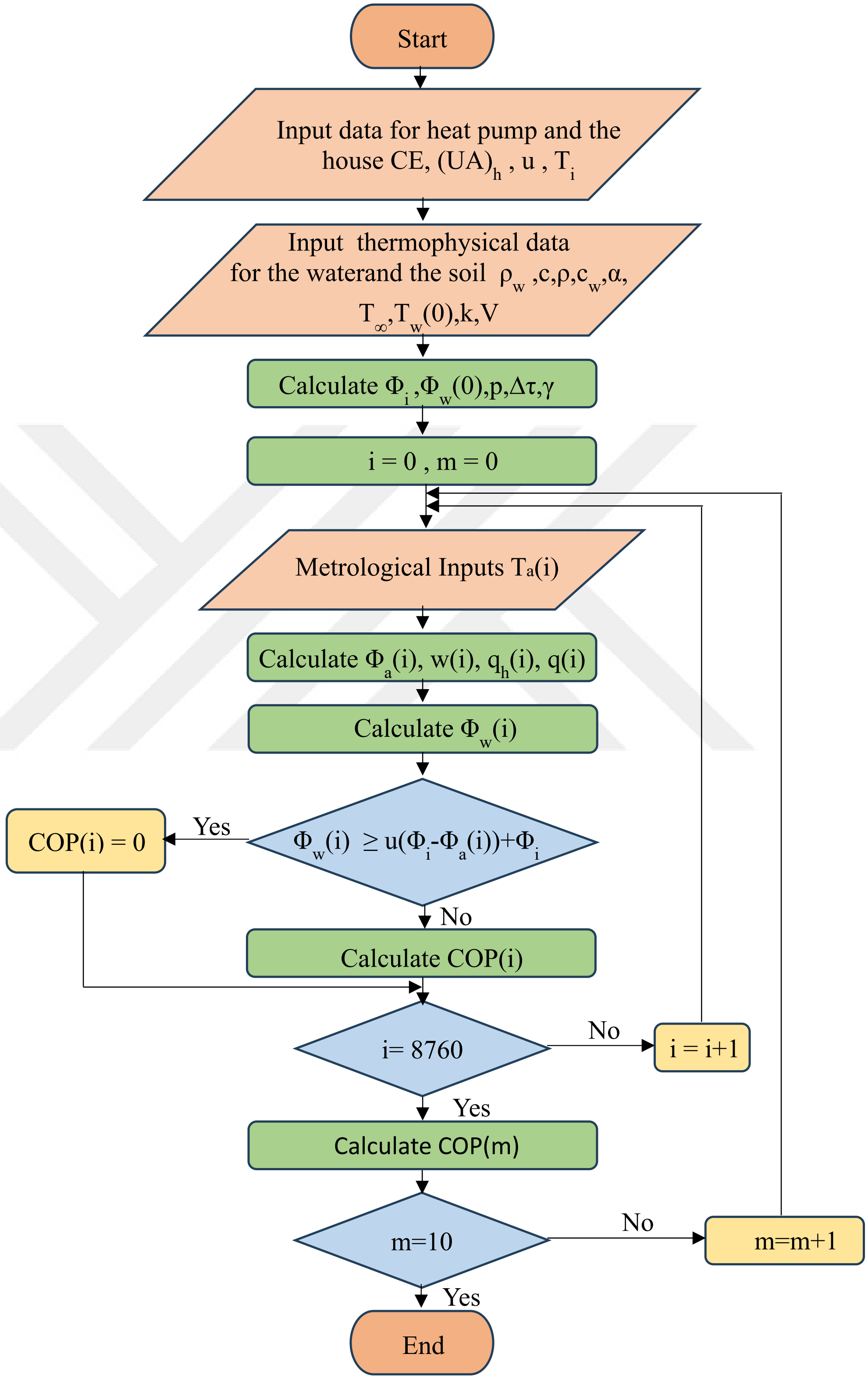

Figure 4.1. Flowchart of MATLAB Code Steps for Heating System connected to an underground TES tank only (Validation Procedure [59]).

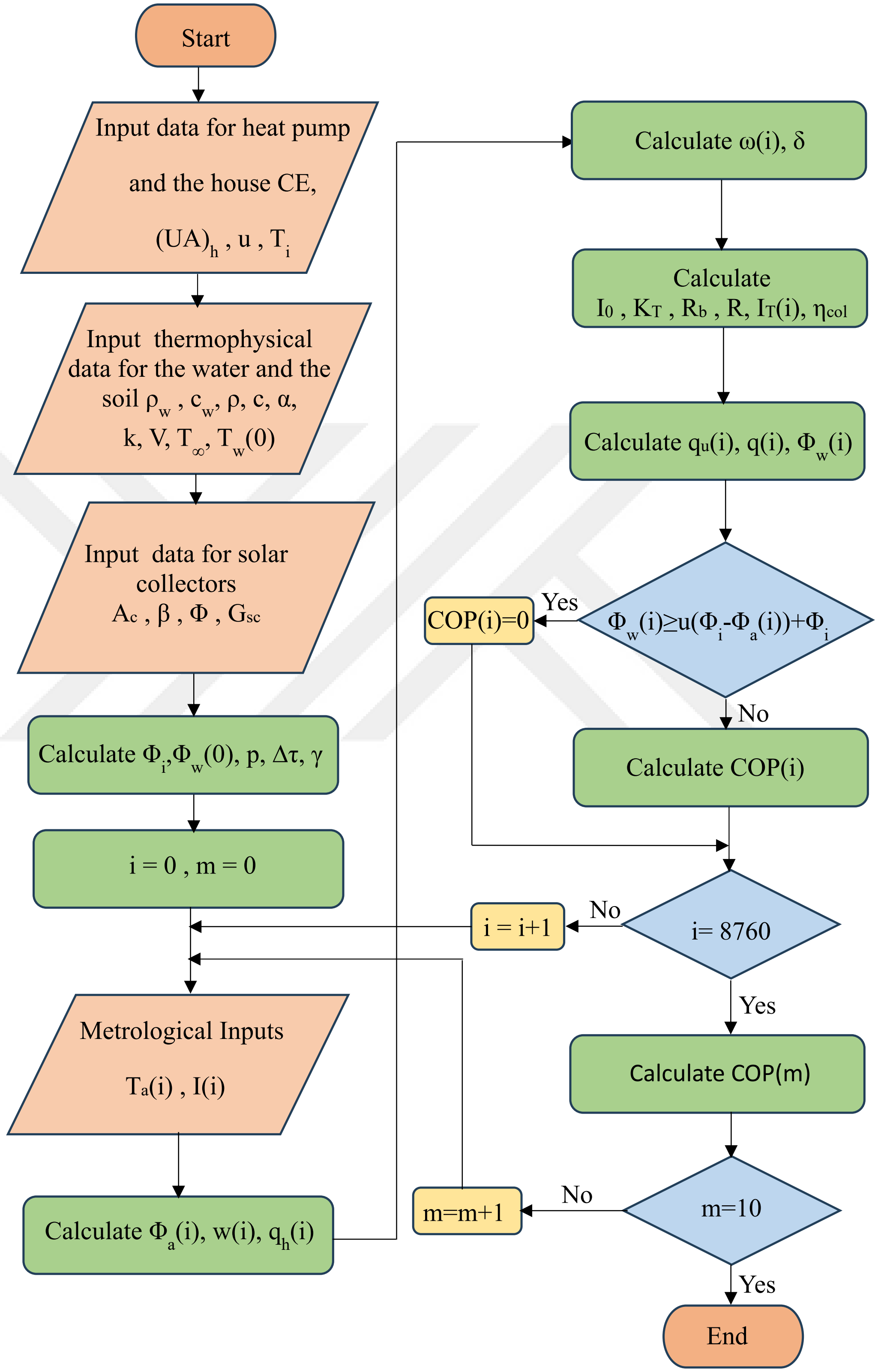

Figure 4.2. Flowchart of MATLAB Code Steps for Heating System connected to an underground TES tank with SC (Validation Procedure [60]).

4.2.1 Validation figures of an underground heat pump system

The obtained figures were compared with those in the study titled (Modeling and performance analysis of a house heating system with a ground-coupled heat pump) [59]. The results from this comparison showed consistency with the findings of the referenced study [59]. Consequently, the MATLAB program utilized for this system has been validated.

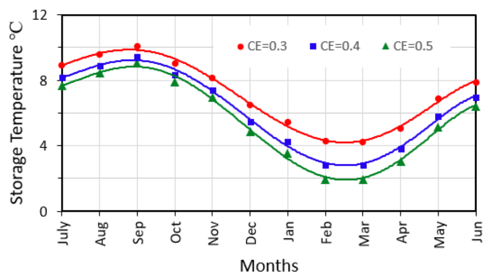

Validated figure

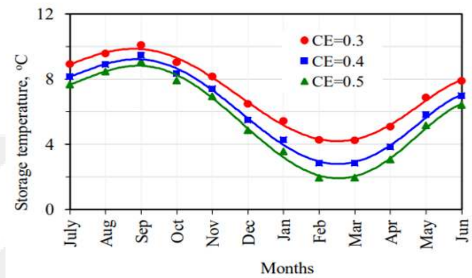

Figure from [59]

Figure 4.3. Effect of CE on the storage temperature during operation time.

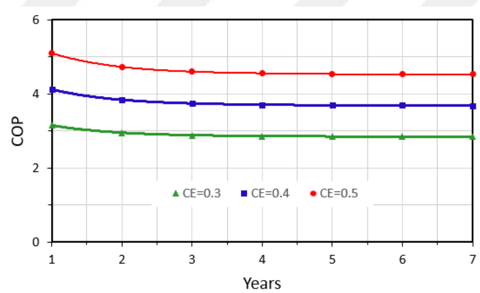

Validated figure

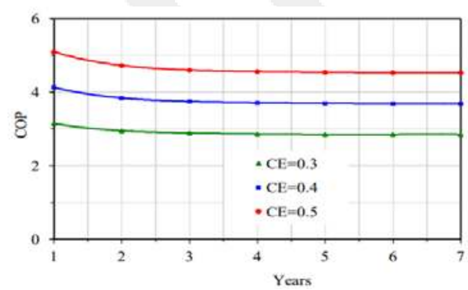

Figure from [59]

Figure 4.4. Effect of CE on the heat pump COP during the seven years.

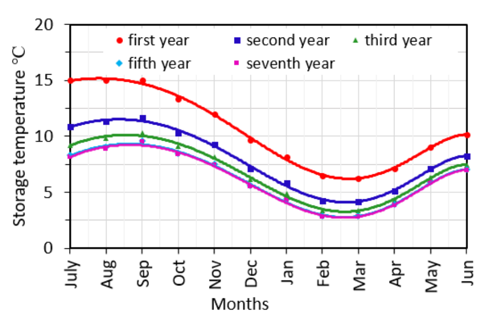

Validated figure

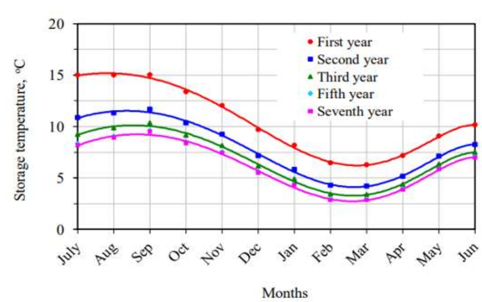

Figure from [59]

Figure 4.5. Variation of TES tank temperature with operation time.

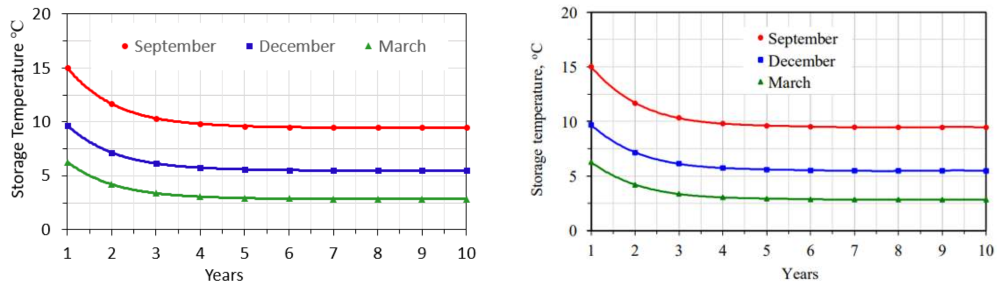

Validated figure　　　　Figure from [59]

Figure 4.6. Variation of storage temperature during ten years.

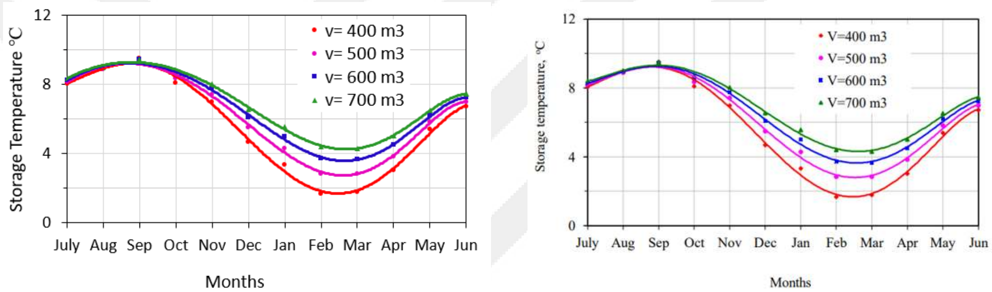

Validated figure　　　　Figure from [59]

Figure 4.7. Variation of annual storage temperature with tank volume during operation time.

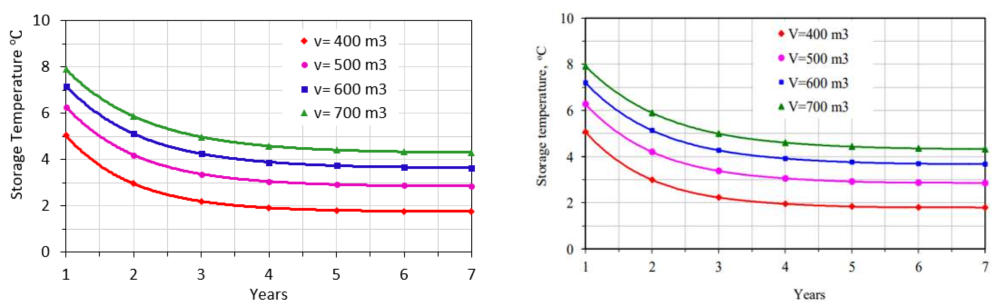

Validated figure　　　　Figure from [59]

Figure 4.8. Variation of storage temperature with operation time during March.

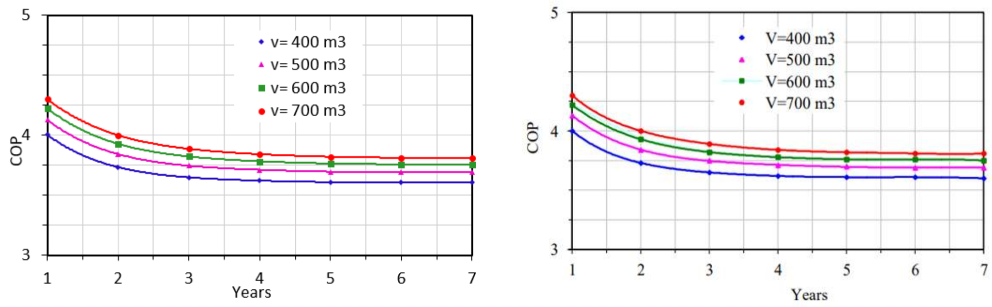

Validated figure Figure from [59]

Figure 4.9. Effect of storage tank volume on the heat pump COP.

4.2.2 Validation figures of the heating system connected to an underground TES tank with using solar collectors

The figures obtained were compared to those presented in the study titled (Energy analysis and modeling of a solar assisted house heating system with a heat pump and an underground energy storage tank) [60]. The comparison showed consistent results, confirming the validity of the MATLAB program used for this system.

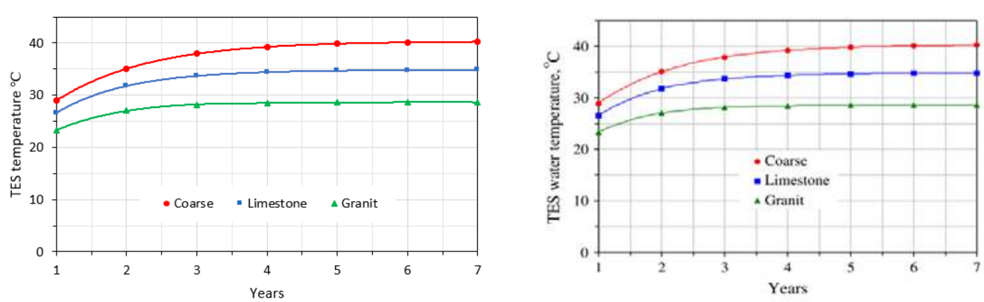

Validated figure Figure from [60]

Figure 4.10. Annual temperature variation of water in the TES tank for Septempe.

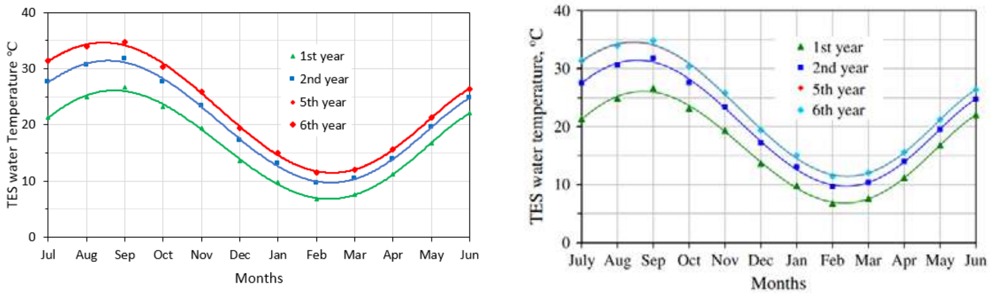

Validated figure

Figure from [60]

Figure 4.11. Annual temperature variation of water in the TES tank with number of operation years

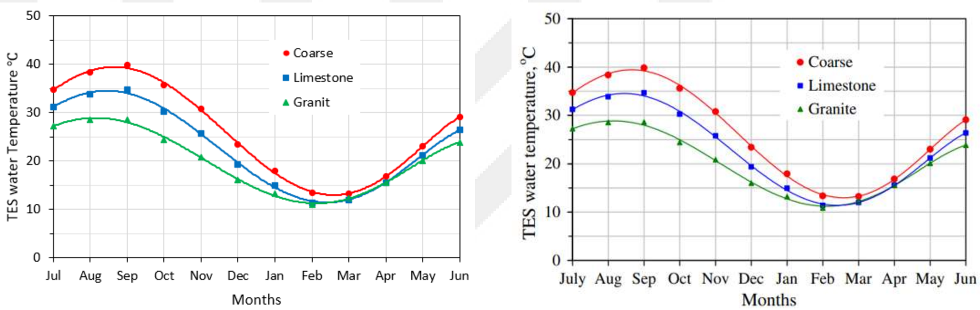

Validated figure

Figure from [60]

Figure 4.12. Effect of earth type on annual temperature variation of water in the TES tank during fifth year of operation

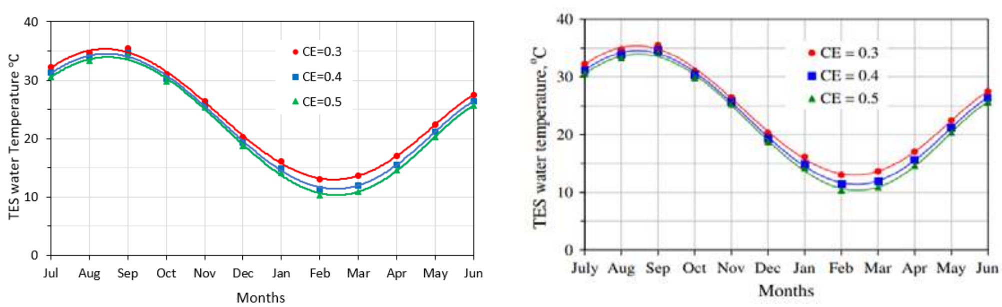

Validated figure

Figure from [60]

Figure 4.13. Effect of CE on annual temperature variation of water in the TES tank during fifth year of operation (limestone, $A_c = 20\ m^2$, $V = 300\ m^3$).

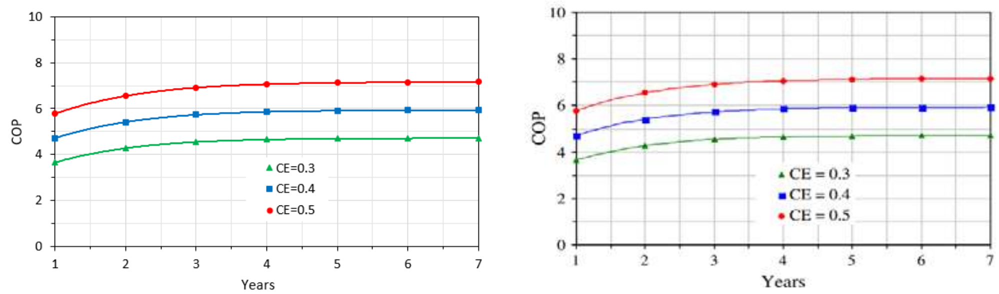

Validated figure Figure from [60]

Figure 4.14. Effect of CE on COP of the heat pump (limestone, A_c = 20 m^2 , V = 300 m^3).

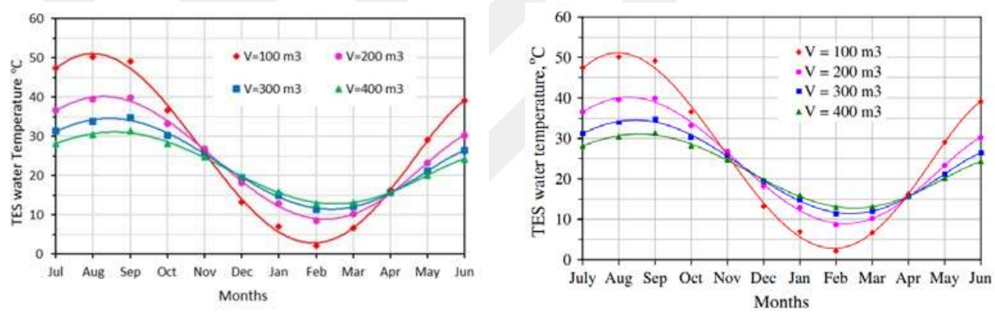

Validated figure Figure from [60]

Figure 4.15. Effect of storage volume on annual temperature variation of water temperature in the TES tank during fifth year of operation (limestone, A_c = 20 m2 , CE = 40%)

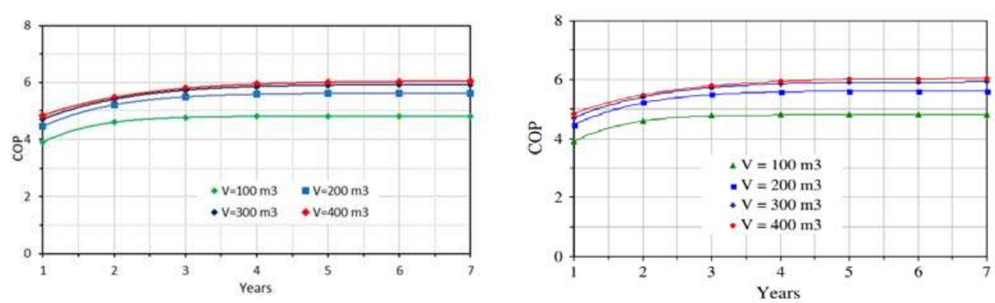

Validated figure Figure from [60]

Figure 4.16. Variation of COP with TES tank volume and operation time (limestone, A_c = 20 m^2 , CE = 40%).

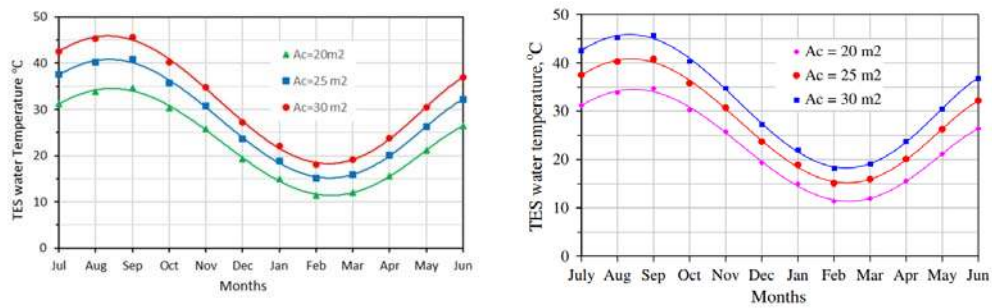

Validated figure   Figure from [60]

Figure 4.17. Effect of collector area on annual temperature of water temperature in the TES tank during fifth year of operation. (limestone, CE = 40%, V = 300 m^3)

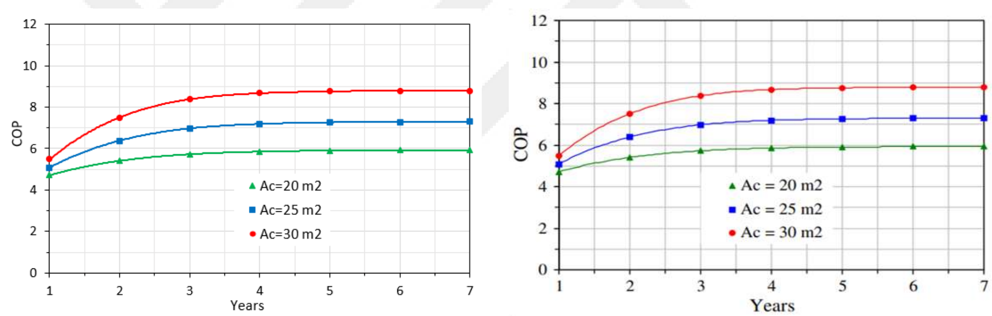

Validated figure   Figure from [60]

Figure 4.18. Effect of collector area on heat pump COP (limestone, CE = 40%, V=300 m^3).

The validation figures presented for the 'Underground Heat Pump System' and the 'Heating System Connected to an Underground TES Tank with Solar Collectors' systems reveal a remarkable conformity. This consistency, where modeled figures closely match those of a previous study conducted under the same specifications, underscores the reliability of the modeling and analysis. The validation figures, as showcased in subsections (4.2.1) and (4.2.2), not only match but also confirm the stability and reliability of the research findings, instilling confidence in the accuracy of the models and the credibility of the insights they offer.

CHAPTER 5
RESULTS AND DISCUSSIONS

In this chapter, this study explores how the Carnot coefficient impacts the performance of a heat pump connected to an underground storage tank with and without using solar collectors. The study examines factors like Carnot efficiency, the volume of the water tank, and the earth type of the surrounding land.

The study also investigates the optimal balance between the tank's volume and the solar collectors' area to maximize system performance. By analyzing these factors, this study aims to uncover insights for improving the design and operation of similar systems. The results were obtained through detailed calculations using MATLAB. The following section provides a comprehensive discussion of these findings and their interpretations.

5.1. Impact of various parameters on the performance of the heating system connected to underground energy storage tank assisted with and without solar collectors

5.1.1 Impact of Carnot efficiency

Figure 5.1. and Figure 5.2. display the impact of the Carnot efficiency CE on tank temperature variations and coefficient of performances in the fifth year of operation for both systems with and without adding SC. Figure 5.1. illustrates the results showcasing the inverse relationship between Carnot Efficiency's values and the tank temperature in the system without SC. As the CE value of the heat pump increases, the water temperature decreases while maintaining a constant heat load. However, in the system connected to solar collectors (SC), the energy gained from solar radiation compensates for the temperature decrease caused by the higher CE.

Consequently, the effect of CE on the tank water temperature is minimal when SC is integrated into the system, highlighting the advantages of incorporating solar collectors into the heating system. Notably, adding SC resulted in a temperature increase in the tank of at least 10.2 °C.

In Figure 5.2., the rise in COP values when solar collectors are added to the heating system is clearly visible, as the values increased by no less than 1.8. It shows that when using a pump with CE = 0.4, the COP value for the system with SC was 4.75 in the first year of operation. The value continued to increase until it settled at approximately 5.41 in the fifth year of operation, While in the system without SC, the COP values continued to decrease for the exact pump specifications after the first year of operation until it settled at approximately 3.6 in the fifth year of operation. An increase in the CE value leads to an increase in the COP value, which leads to an increase in the amount of heat extracted from the tank Q_L for the same required heat load Q_H; therefore, the tank's temperature decreases.

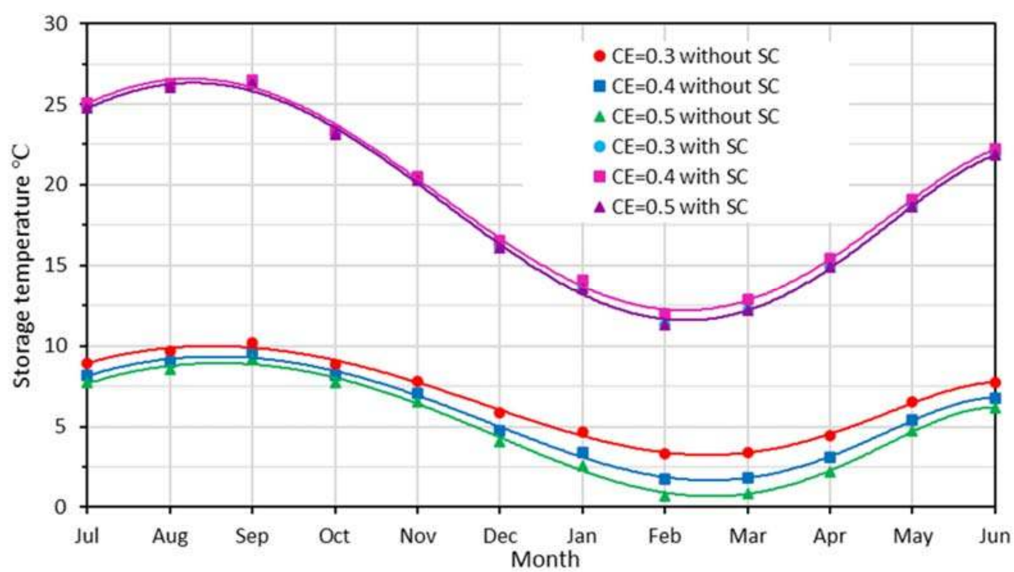

Figure 5.1. The effect of CE on the annual variation of water temperature in the TES tank in the fifth year of operation. (v=400 m^3, granite)

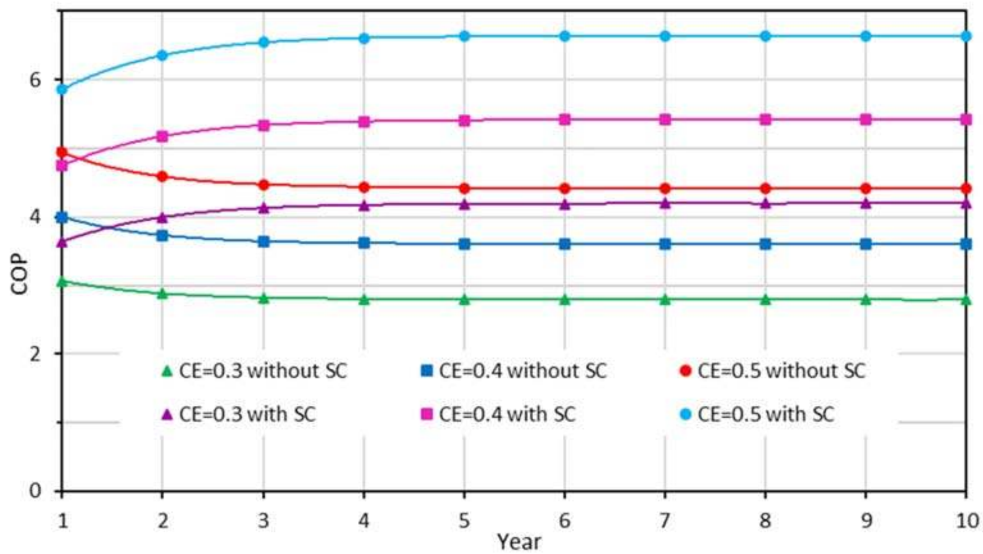

Figure 5.2. The effect of CE on the COP of the heat pump. (v=400 m^3, Granite)

5.1.2 Impact of the volume of the storage tank

The relationship between the volume of the storage tank surrounded by the Earth and the thermal conductivity of the earth is an essential element in the design and performance of heating systems based on thermal energy storage.

The volume of the storage tank enclosed by the Earth determines the amount of thermal energy that can be stored. It, therefore, affects the system's operation period and its sustainability. In general, the larger the tank's volume, the greater its ability to hold more heat. This can lead to an increase in the period of heat availability in the system and reduce the dependence on additional energy.

Figure 5.3. shows the effect of the tank's volume on the water temperatures of the tank, as the results show a slight effect of it, especially in the heating season, for volumes that exceed 300 m^3. However, it is also clear that using volumes below 300 m^3 is ineffective for the system without SC, as the results approached zero degrees and reached below zero when using a tank of 200 m^3.

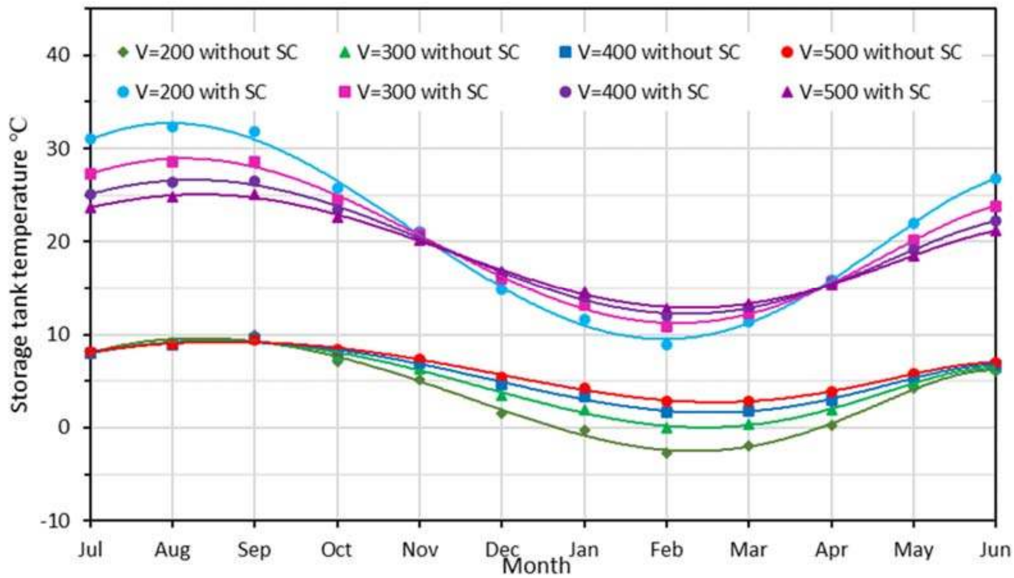

Figure 5.3. Effect of storage tank volume on the annual temperature variation of water temperature in the TES tank during tenth year (Granite, CE=0.4).

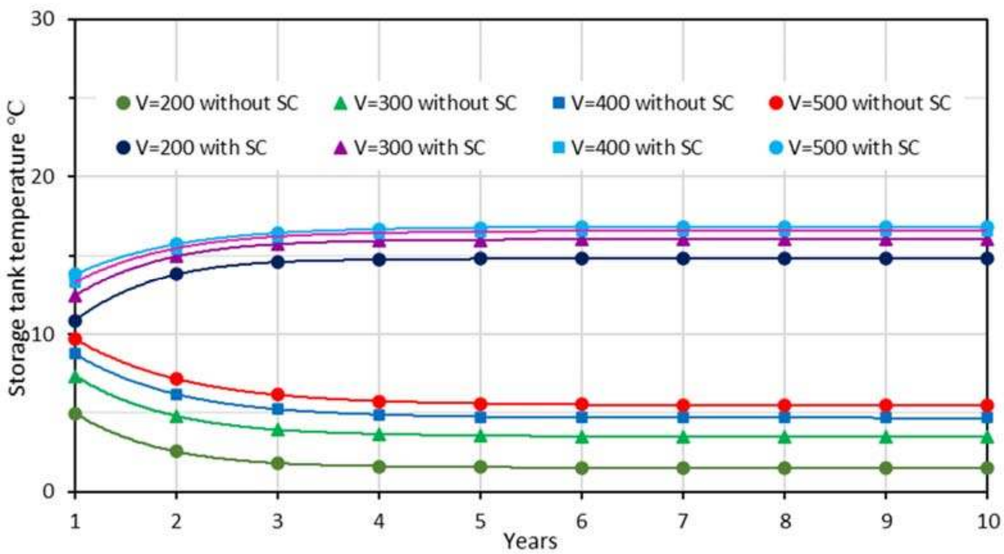

Figure 5.4. Variation of the water temperature in the TES tank with TES tank volume and operation time (Granite, CE=0.4, December).

Figure 5.4. illustrates the annual tank temperatures in the system with and without solar collectors (SC) in December. It shows a steady increase in the system with SC until it reaches a constant value after the fifth year of operation, indicating stabilization. In contrast, the temperatures in the other system initially decreased after the first year of

operation and also stabilized at a constant value after the fifth year. These observations indicate that both systems exhibit annual periodic operational conditions. The system incorporating solar collectors experiences an increase in tank temperatures over time, while the other system experiences a decrease followed by stabilization.

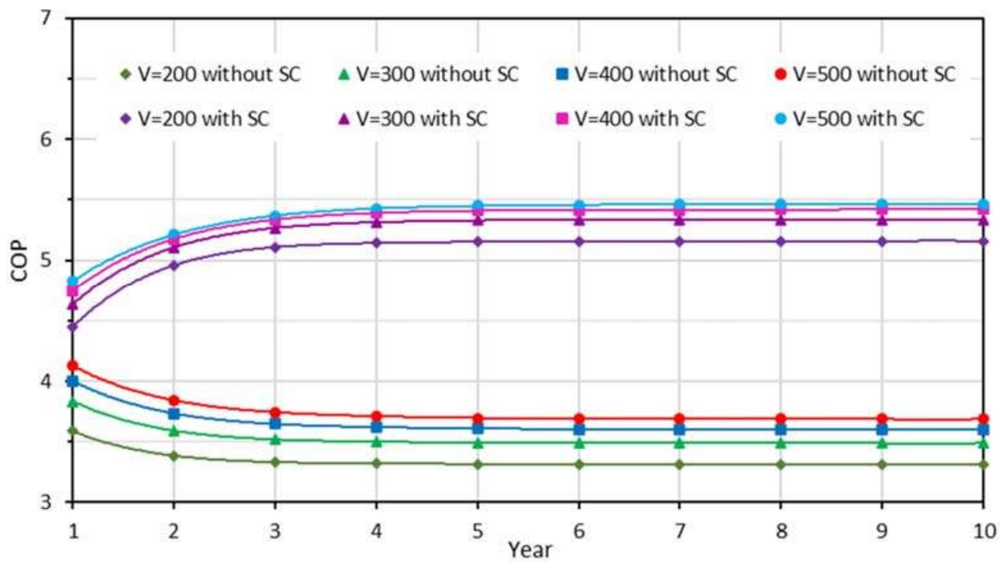

Figure 5.5. Variation of COP with TES tank volume and operation time (Granite, CE=0.4).

Figure 5.5. shows the effect of the volume of the tank on COP, where it is shown that the larger the volume, the higher the COP value for both systems. From the energy balance of the storage tank, we know that increasing the volume of the tank means increasing the amount of sensible energy of the water times the amount of energy lost through thermal conductivity, and thus increasing the net energy of the tank Eq. (3.14), which is the heat source of the heat pump. This increase leads to an increase in the COP of the heat pump for the same required heat load (sink).

The second observation in Figure 5.5. is that at the beginning of the operation, the tank volume of 500 m^3 recorded the highest COP value in both systems, as the COP value in the system with SC in the first year of operation was 4.8 and continued to increase until it stabilized in the fifth year at approximately 5.45. Also, in the system without SC, the tank volume of 500 m^3 recorded the highest value of COP in the first year of operation at the value of 4.1. Still, it continued to decrease until it stabilized at a value of 3.7 in the fifth year of operation. The addition of SC to the system compensates for the decrease in the temperature of the tank water, which helps to increase the COP value in the first years of operation, unlike what happened in the other system.

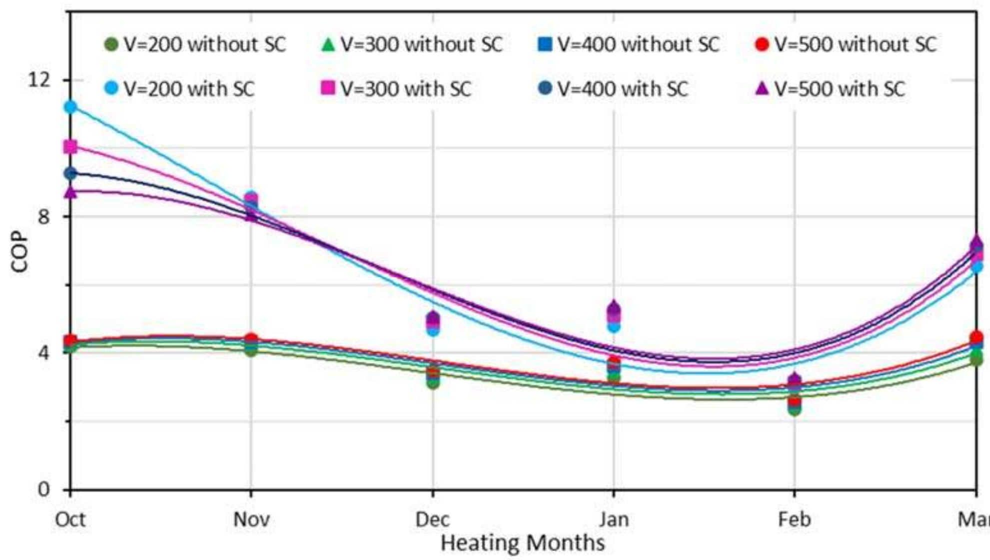

Figure 5.6. Effect of storage tank volume on the annual variation of COP during the tenth year in heating months (Granite, CE=0.4).

Figure 5.6. shows the effect of changing the tank's volume on the COP values during the heating season and in the tenth year of operation. In the system without solar collectors, the tank's volume had no significant effect after ten years of operation, as the increase in COP was very slight, and the values had a smooth variation throughout the months of heating. As for the system that contains solar collectors, the COP values decreased at the beginning of the heating season in October and reached the lowest value in January and February, with a slight improvement in the COP values with increasing the volume of the tank. To compare the two systems with each other, when solar collectors were added to the system, the COP values increased to no less than 4.4 in October of operation and up to 0.66 in February.

5.1.3 Impact of the earth type surrounding the storage tank

In addition to the volume of the storage tank, the thermal conductivity between the tank and the soil plays an essential role in transferring heat between them. Thermal conductivity depends on factors such as soil quality and tank surface area. The greater the thermal conductivity, the more efficiently the system can use the heat stored in the ground. Furthermore, soils are usually different thermal conductors, as some soils can be more heat-conductive than others. Thus, the earth type affects the heat transfer rate between the tank and the soil, which in turn affects the system's efficiency and performance.

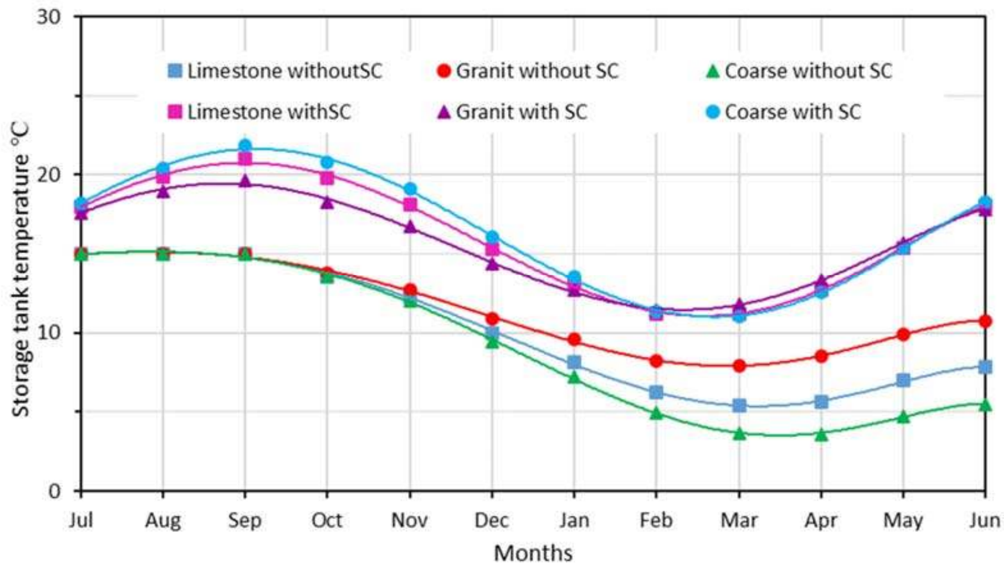

Figure 5.7. The effect of earth type on T_w in the first year of operating with V = 700 m3 and CE = 0.4.

Figure 5.7. demonstrates the influence of different types of Earth on the temperature of the storage tank in both systems. The impact was more pronounced in the system without solar collectors (SC), where the type of Earth, mainly granite with the highest thermal conductivity coefficient (Table 4.), resulted in the most elevated temperatures during cold months compared to other soil types. This is because the tank primarily relies on heat acquired from the surrounding Earth, and higher thermal conductivity coefficients lead to increased heat conduction. In the system with SC, the effect of Earth type was less significant. The tank's most elevated temperatures were observed with coarse soil with the lowest conductivity coefficient. This characteristic allows the tank to retain heat gained from solar collectors. After the cold winter months, the tank utilizes both Earth's heat and solar radiation, explaining why coarse soil recorded the lowest temperatures in March and April despite a slight temperature difference compared to other soil types.

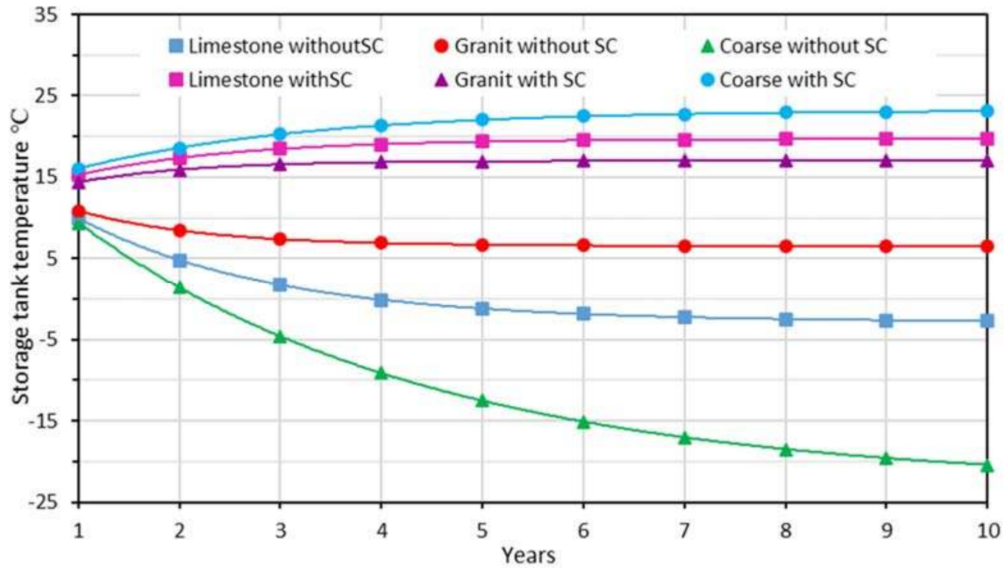

Figure 5.8. The effect of earth type on T_w in ten years of operating with V = 700 m^3 and CE = 0.4.

Figure 5.8. illustrates the impact of different types of Earth on the annual water temperature of the tank. In the system with solar collectors (SC), it is observed that the temperature values experienced an increase after the first year of operation. The tank temperature started at 16°C in the first year and continued to rise until stabilizing at approximately 23°C after the seventh year of operation. This increase is attributed to the presence of coarse soil, which has a low thermal conductivity coefficient. The low conductivity coefficient allows the tank to retain heat gained from solar collectors, gradually increasing temperature over time.

On the other hand, in the system without solar collectors, granite soil exhibited stable and decreased temperatures over the years of operation. The periodic operating temperature stabilized at 6.5°C after the fifth year. However, both coarse and limestone soils recorded a sharp temperature drop to below zero. This drop in temperature is due to their low thermal conductivity coefficient, which limits the tank's ability to compensate for heat loss during cold months that would typically be gained from the surrounding ground.

In summary, the type of Earth has a notable influence on the annual water temperature of the tank, with the system containing solar collectors benefiting from the heat retention capability of coarse soil. In contrast, the system without solar collectors experiences temperature stability in granite soil but encounters significant temperature drops in coarse and limestone soils.

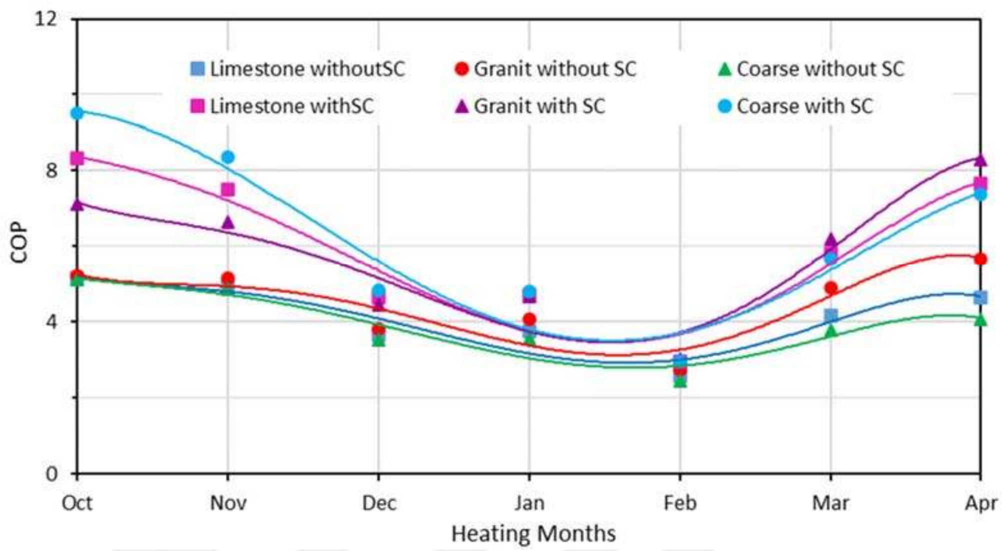

Figure 5.9. Variation of COP with earth type and operation time (Granite,CE=0.4).

Figure 5.9. illustrates that the coarse soil type achieved the highest COP value of 9.5 in October. After that, however, the COP value started to decrease and reached 2.9 in the February before rising again. Coarse is characterized by a low coefficient of thermal conductivity, and therefore the heat of conduction with the surrounding Earth is low, which makes the amount of heat extracted from the storage tank and gained from solar energy is higher than the other soil types.

With the beginning of the heating months, the heat of the tank, which was obtained in the summer season, is consumed. With a decrease in the conductivity coefficient of the Earth, it is difficult for the tank to compensate for the lack of heat from the surrounding heat, which leads to a decrease in the amount of heat extracted from the tank, and as the heating months progress, the values of cop decrease, where the relationship between COP and the amount of heat removed from the tank is a direct relationship (Eq. 3.34). After the month of February, the cop values return to rise, taking advantage of the heat of solar radiation and taking advantage of the heat of the Earth, so it is noticed from Figure 5.9. that the COP values of Granite are higher at the end of the heating season, as Granite is characterized by a high conductivity coefficient compared to the other two types of soil.

It is also noted from the figure that the COP values in the system with SC and the months of October and November rise by at least (1.5) and the values in the cold winter months (December - January - February) converge with the values obtained by the other system, the difference between them does not exceed (0.5) in February.

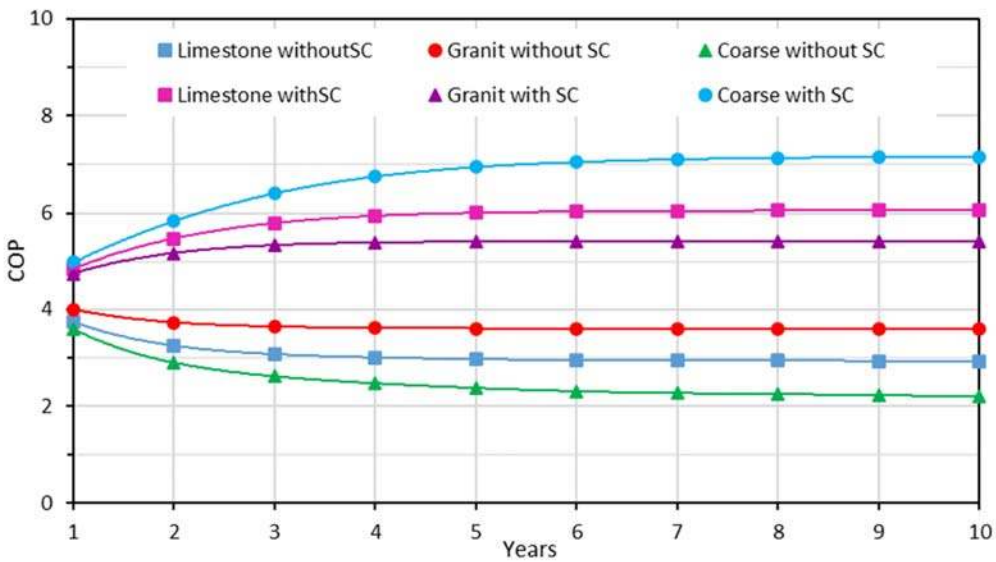

Figure 5.10. The effect of earth type on COP in ten years of operating with V= 400 m^3 and CE = 0.4.

Unlike the variations observed in the previous figure, the COP values in Figure 5.10. exhibit a consistent trend over the years of operation, either increasing in the system with solar collectors (SC) or decreasing in the other system.

The results depicted in Figure 5.8. indicate that the lower thermal conductivity and thermal diffusivity coefficients of the soil surrounding the thermal storage tank contribute to a higher coefficient of performance in the system with SC. The lower thermal conductivity coefficient slows down heat transfer, allowing the storage tank to maintain the temperature obtained from solar energy for an extended period. This positively impacts the efficiency of the heat pump.

Conversely, in the system without solar collectors, the decrease in thermal conductivity and thermal diffusivity coefficients of the surrounding soil reduces its ability to transfer heat to the storage tank. Thus, the coefficient of performance (COP) of the heat pump decreases, as illustrated in Figure 5.10.

5.1.4 Monthly and annually periodic conditions of the system's parameter

The results of this study were analyzed and discussed based on the monthly and annual operating conditions. The discussion focused on the temperature of the tank and the coefficient of performance (COP) of the system under different conditions.

It is evident from Figure 5.11. that the tank temperatures follow a consistent pattern throughout the year when the variables associated with the pump and storage tank remain constant. The highest temperatures are observed before the start of the heating season, while the lowest temperatures are recorded during the colder months of January and February. After the fifth year of the operation, the system reaches a state of periodic operating conditions where temperature fluctuations in the tank remain relatively constant across the years in both systems. This is supported by Figure 5.12, which depicts changes in the coefficient of performance COP during the heating months over multiple years.

The figure demonstrates the stability of COP values after the fifth year of the operation in the both systems. Furthermore, it is noticeable that the lowest COP values occur during the cold heating months of December, January, and February. In terms of COP variability throughout the year, the system without solar collectors exhibits a more stable pattern compared to the other system.

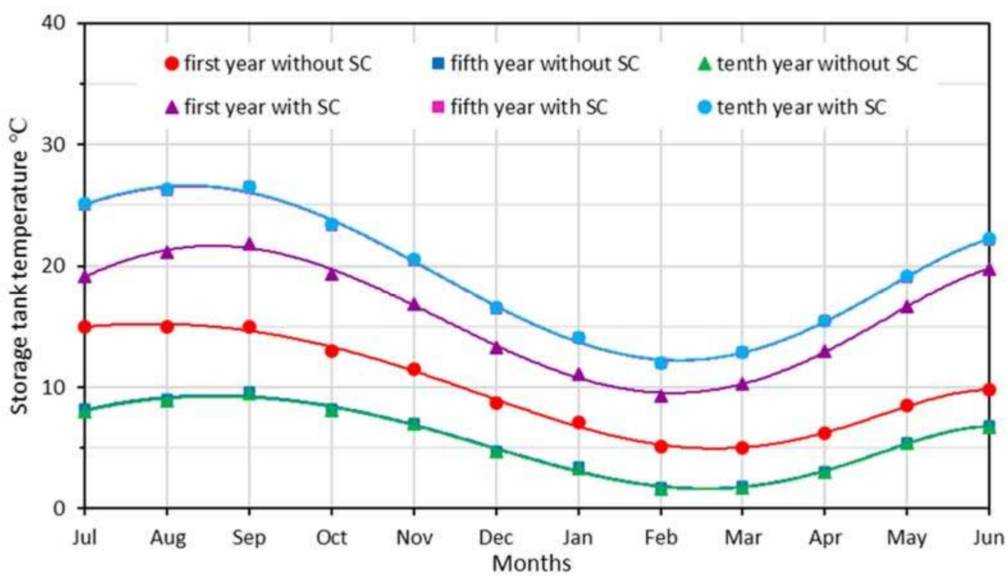

Figure 5.11. Annual temperature variation of water in the tank with number of operation years considering Granite, V = 400 m^3 and CE = 0.4.

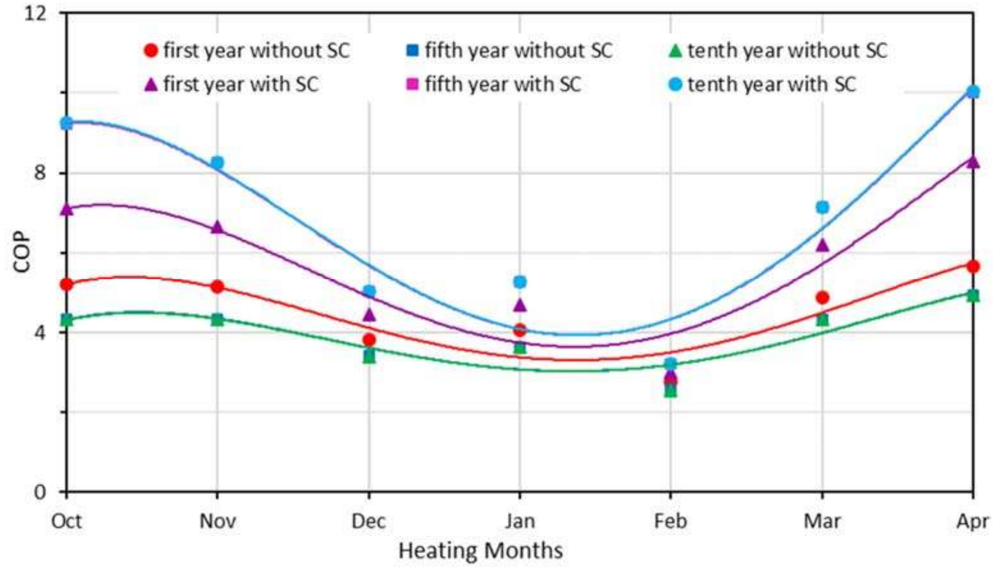

Figure 5.12. Annual variation of COP with number of operation years considering the earth type of Granite, V = 400 m^3 and CE = 0.4.

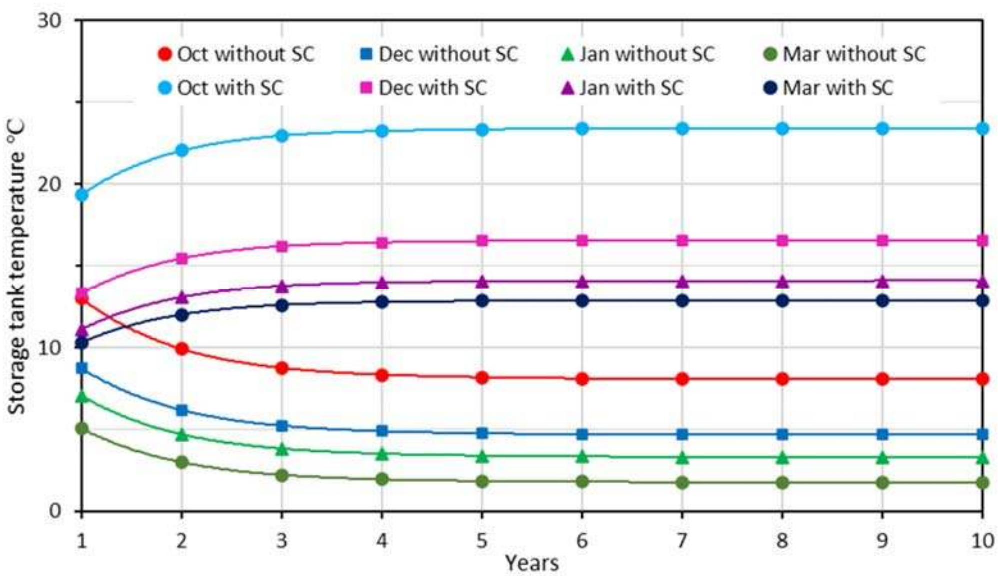

Figure 5.13. Variation of water temperature of the tank in ten operation years with heating months considering Granite, V = 400 m^3 and CE = 0.4.

To investigate the long-term behavior of the system, a comprehensive analysis was conducted to study the variations in water temperature and coefficient of performance (COP) over multiple years. This long-term analysis provides valuable insights into the overall trends and patterns exhibited by these parameters throughout the studied period. In addition, by examining the annual variations, a more comprehensive understanding of the system's performance and its changes over time can be obtained.

Figures 5.13. and 5.14. confirm what the results showed in the previous figures, where the COP recorded the highest value in October, the lowest value in the cold months, and stability in annual Values after the fifth year of the operation, as well as the temperature change of the tank.

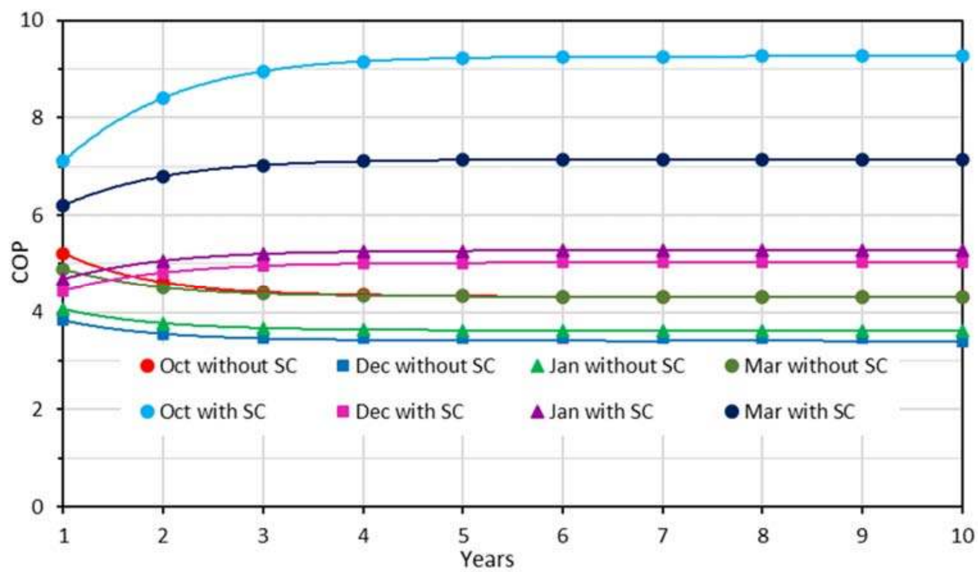

Figure 5.14. Variation of COP in ten operation years with heating months. (Granite, V = 400 m^3 and CE = 0.4)

These results demonstrate the importance of studying and analyzing the monthly and annual operating conditions on the tank temperature and the coefficient of performance of the heat pump system connected to a ground tank and solar collectors. In addition, this discussion helps to understand how the surrounding conditions affect the system's performance and provide appropriate solutions to improve its efficiency and sustainability.

5.2 Solar collector area to storage tank volume ratio for enhanced performance of the heating system connected to underground energy storage tank assisted with solar collectors

One critical aspect of optimizing the performance of such a hybrid system is determining the ideal ratio between the area of solar collectors and the volume of the underground storage tank. This ratio plays a pivotal role in harnessing and utilizing solar energy effectively, ultimately impacting the coefficient of performance (COP) of the heat pump system. Achieving an optimal balance between collector area and storage tank volume can significantly enhance the system's energy efficiency and economic viability.

To determine the optimal ratio between solar collector area (Ac) and storage tank volume (V), we conducted a series of simulations and experiments while keeping other system parameters constant, such as the type of earth and Carnot efficiency of the heat pump.

Figure 5.15 illustrates the relationship between COP and solar collector area at various tank volumes. The figure reveals that the optimal collector area, resulting in the highest coefficient of performance (COP), is 30 m^2, corresponding to a tank volume of 200 m^3. This yields a ratio of 0.15, as demonstrated in Figure 5.16, which also presents the relationship between COP and the (A_c /V) ratio. The Results indicate that, for a 10 kW heat load, the most effective configuration for achieving the highest COP value consists of a 200 m^3 tank and a 30 m^2 solar collector area. Additionally, Figure 5.16 highlights that when dealing with a 10 kW heat load, utilizing collector areas exceeding 30 m^2 in conjunction with tank volumes exceeding 200 m^3 does not confer significant additional benefits to the system.

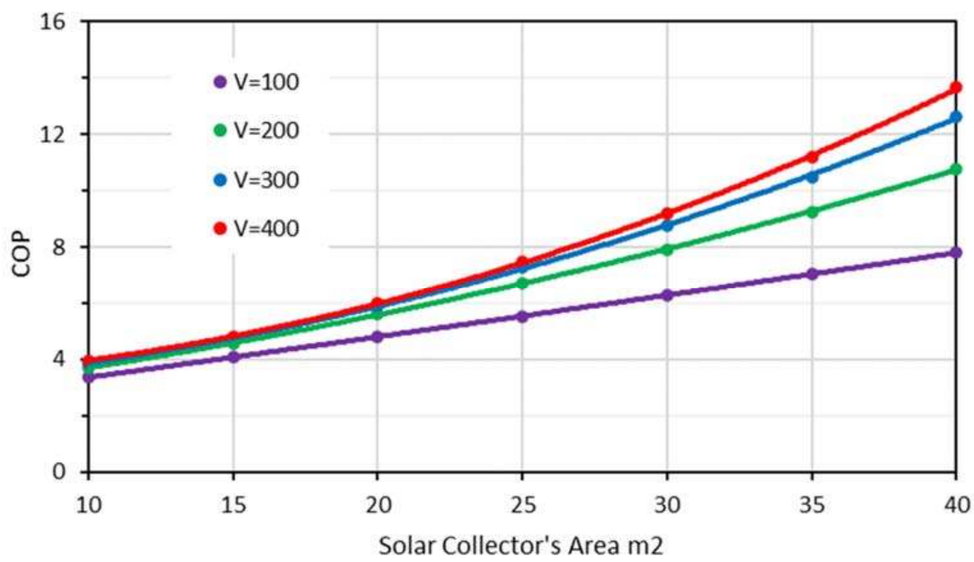

Figure 5.15. COP variation with solar collector area for different storage tank volumes.

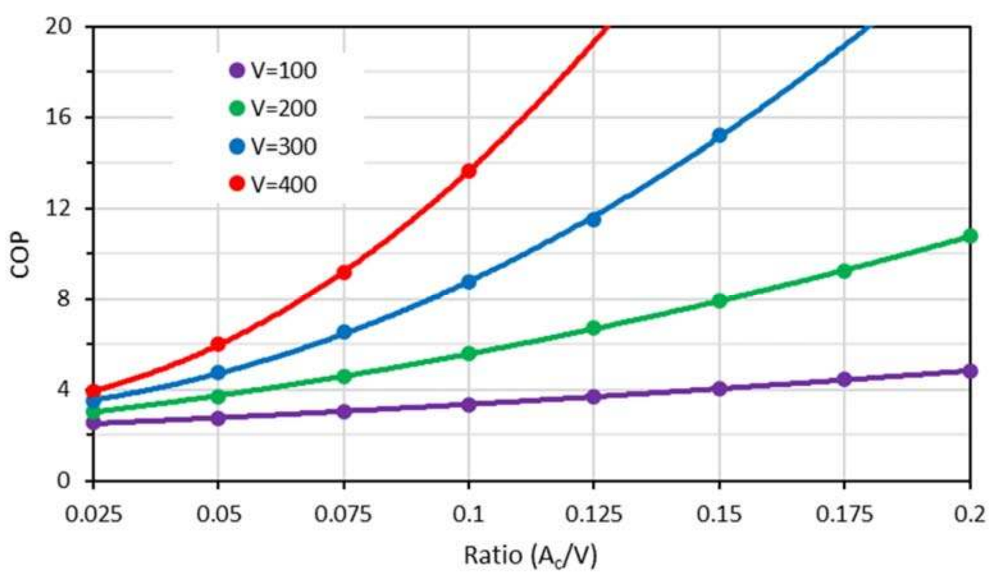

Figure 5.16. COP variation with solar collector area to storage tank volume ratio

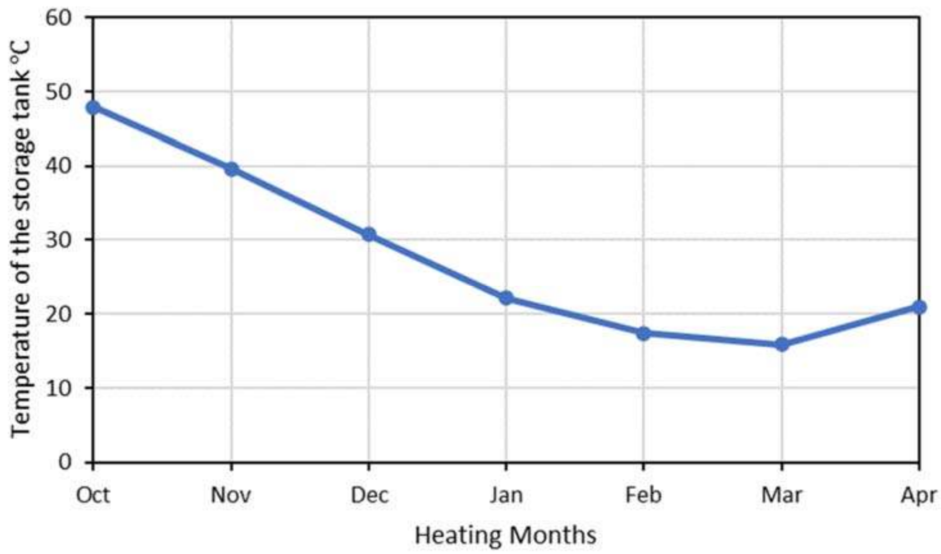

Figure 5.17. Temperature Values of the storage tank in Optimal solar collector area to storage tank volume ratio.

To comprehend the impact of the optimal ratio between tank volume and solar collector area on the heating system, Figure 5.17 illustrates the variations in the tank's temperature throughout an entire heating season, with Ac=30 m^2 and V=200 m^3, for a house with a 10 kW heat load. These observations emphasize the critical importance of considering this factor when designing and operating hybrid systems of this nature. Such consideration has the potential to significantly enhance the efficiency and environmental friendliness of these systems.

CHAPTER 6
CONCLUSION

This thesis involved conducting a thorough analysis of two heat pump systems: one linked to an underground storage tank and the other integrated with an underground storage tank alongside solar collectors. The objective was to evaluate these systems' performance under various operational conditions. The study specifically concentrated on two vital parameters - tank temperature and coefficient of performance (COP) - to gauge the systems' efficiency and sustainability. By exploring monthly and annual variations, valuable insights were gleaned regarding the systems' behavior over time. The subsequent points present a concise summary of the main findings and their potential implications for enhancing the performance of comparable systems:

1. The addition of solar collectors (SC) resulted in a significant temperature increase in the tank of at least 10.2 °C. Additionally, it led to an increase in the coefficient of performance (COP) by at least 1.8. These improvements were observed for a tank volume of 400 m^3, a pump with a Carnot coefficient of 0.4, and when using granite as the surrounding of the tank.
2. The increase in the Carnot efficiency positively affected the coefficient of performance of both systems. However, its impact on the tank temperature was negligible in the system with solar collectors.
3. The tank volume had a mild effect on the tank temperatures in both systems, particularly for volumes above 300 m^3. It was found that using a tank with sizes less than 300 m^3 in a system without solar collectors was ineffective. Similarly, the effect of increasing the tank volume on the coefficient of performance was minor in both systems.
4. When incorporating solar collectors into the heating system, it is advisable to utilize soils with low thermal conductivity. This choice helps maintain high temperatures in the tank and achieve the highest values of the system's performance coefficient.

5. Over time, both systems show stable COP values. The system with solar collectors has higher COP values. The analysis of tank temperature and COP values over several years reveals consistent patterns and stability after the fifth year of operation.
6. Through simulations and experiments, the study determined the optimal ratio for achieving the highest COP. For a 10 kW heat load, the optimal configuration entails a 30 m^2 collector area and a 200 m^3 tank volume, resulting in a ratio of 0.15.
7. Beyond this ideal configuration, the results demonstrate that increasing collector areas beyond 30 m^2 and tank volumes beyond 200 m^3 does not yield significant additional benefits for a 10 kW heat load.
8. The significance of the optimal ratio is further illustrated by variations in the tank's temperature throughout a heating season. This emphasizes the crucial factor of considering this ratio in the design and operation of such hybrid systems.

Incorporating these findings into the design and operation of hybrid heating systems utilizing solar collectors and underground energy storage tanks has the potential to yield substantial enhancements in both energy efficiency and environmental sustainability. To conclude, in light of the insights gained from this study, we recommend further research in the domain of hybrid thermal systems. Such investigations can explore optimal configurations and outcomes, thereby fostering advancements in this field.

REFERENCES

[1] A.H. Al-Badi, M.H. Albadi, (2012). Domestic solar water heating system in Oman: Current status and future prospects, Renewable and Sustainable Energy Reviews, 16, 5727-5731.

[2] C. Zhou, E. Doroodchi, B. Moghtaderi, (2013). An in-depth assessment of hybrid solar–geothermal power generation , Energy Conversion and Management , 74 , 88-101.

[3] D. Moya, C. Aldás, P. Kaparaju, (2018). Geothermal energy: Power plant technology and direct heat applications, Renewable and Sustainable Energy Reviews , 94 , 889-901.

[4] K. Li, H. Bian, C. Liu, D. Zhang, Y. Yang, (2015). Comparison of geothermal with solar and wind power generation systems , Renewable and Sustainable Energy Reviews , 42 , 1464-1474.

[5] A. V. Novo, J. R. Bayon, D. Castro-Fresno, J. Rodriguez-Hernandez, (2010). Review of seasonal heat storage in large basins: Water tanks and gravel–water pits, Applied Energy, 87, 390–397.

[6] X. Zhou, Y. Xu, X. Zhang, D. Xu, Y. Linghu, H. Guo, Z. Wang, H. Chen, (2021). Large scale underground seasonal thermal energy storage in China , Journal of Energy Storage , 33 , 102026.

[7] A. Q. Abdullah, (2021). Selection and Modelling Study on High-Temperature Thermal Energy Storage for Industrial Purposes (Master's thesis, Eindhoven University of Technology).

[8] I. Dincer, S. Dost, X. Li, (1997). Performance analyses of sensible heat storage systems for thermal applications, International Journal Of Energy Research, 21 , 1157—1171.

[9] Thomas Bauer, Nicole Pfleger, Nils Breidenbach, Markus Eck, Doerte Laing, Stefanie Kaesche, (2013). Material aspects of Solar Salt for sensible heat storage, Applied Energy, 111, 1114-1119.

[10] S. Jegadheeswaran, Sanjay D. Pohekar, (2009). Performance enhancement in latent heat thermal storage system: A review, Renewable and Sustainable Energy Reviews, 13, 2225-2244.

[11] E. G. Jung, J. Hong Boo , (2014). Thermal analytical model of latent thermal storage with heat pipe heat exchanger for concentrated solar power, Solar Energy, 102, 318-332.

[12] S. Kalaiselvam, R. Parameshwaran, (2014). Thermal Energy Storage Technologies for Sustainability: Systems Design, Assessment and Applications, Academic press.

[13] Aynur Ucar , Mustafa Inalli, (2008). Thermal and economic comparisons of solar heating systems with seasonal storage used in building heating, Renewable Energy, 33, 2532– 2539.

[14] Dincer I, Rosen MA. Thermal energy storage—systems and applications. New York, US: John Wiley & Son; 2002.

[15] H. Huanga, Y. Xiaoa, J. Lin, T. Zhoua, Y. Liua, Q. Zhao, (2019). Thermal characteristics of a seasonal solar assisted heat pump heating system with an underground tank, Sustainable Cities and Society, DOI: https://doi.org/10.1016/j.scs.2019.101910.

[16] H. Caliskan, I. Dincer , A. Hepbasli, (2012). Thermodynamic analyses and assessments of various thermal energy storage systems for buildings, Energy Conversion and Management, 62, 109-122.

[17] M.C. Rodríguez-Hidalgo, P.A. Rodríguez-Aumente, A. Lecuona, M. Legrand, R. Ventas, (2012). Domestic hot water consumption vs. solar thermal energy storage: The optimum size of the storage tank, Applied Energy, 97, 897-906.

[18] R. Yumrutas,, M. Kunduz, T. Ayhan, (2003). Investigation of thermal performance of a ground coupled heat pump system with a cylindrical energy storage tank, International Journal of Energy Research, 27, 1051–1066.

[19] M. Chung, J. Park* And H. Yoon, (1998). Simulation Of A Central Solar Heating System With Seasonal Storage In Korea, Solar Energy, 64, 163-178.

[20] H.-F. Zhang, X.-S. Ge, H. Ye, (2007). Modeling of a space heating and cooling system with seasonal energy storage, Energy, 32, 51-58.

[21] Y.H. Kuang, R.Z. Wang, L.Q. Yu, (2003). Experimental study on solar assisted heat pump system for heat supply, Energy Conversion and Management, 44, 1089–1098.

[22] H. Wang, C. Qi, (2008). Performance study of underground thermal storage in a solar-ground coupled heat pump system for residential buildings, Energy and Buildings, 40,1278–1286.

[23] M. Qu, H Yin, D. H. Archer, (2010). A solar thermal cooling and heating system for a building: Experimental and model based performance analysis and design, Solar Energy, 84, 166–182.

[24] R. Yumrutaş, M. Ü nsal , (2000). Analysis of solar aided heat pump systems with seasonal thermal energy storage in surface tanks, Energy, 25, 1231–1243.

[25] M. Inallı, (1998). Design parameters for a solar heating system with an underground cylindrical tank, Energy, 23, 1015–1027.

[26] Y. Zhang, G. Zhou, K. Lin, Q. Zhang, H. Di, (2007). Application of latent heat thermal energy storage in buildings: state-of-the-art and Outlook, Building and Environment, 42, 2197–209.

[27] O. Hoes, M. Trcka, JLM. Hensen, B. H. Bonnema, (2011). Investigating the potential of a novel low-energy house concept with hybrid adaptable thermal storage. Energy Conversion and Management, 52, 2442–7.

[28] D. Vanhaudt, J. Desmedt, J. Van Bael, N. Robeyn, H. Hoes, (2011). An aquifer thermal storage system in a Belgian hospital: longterm experimental evaluation of energy and cost savings, Energy and Buildings, 43, 3657–65.

[29] J. Kim, Y. Lee, W. S. Yoon, J. S. Jeon, M. H. Koo, Y. Keehm, (2010). Numerical modeling of aquifer thermal energy storage system, Energy, 35, 4955-65.

[30] E. Mohamed, S. Riffat, S. Omer, (2017). Low-temperature solar-plates-assisted heat pump: A developed design for domestic applications in cold climate, Refrigeration, 81, 134-150.

[31] Z. Han, C. Bai, X. Ma, B. Li, H. Hu, (2018). Study on the performance of solar-assisted transcritical CO_2 heat pump system with phase change energy storage suitable for rural houses, Solar Energy, 174, 45-54.

[32] S. Qu, F. Ma, R. Ji, D. Wang, L. Yang, (2015). Energy and Buildings, 105, 294-301.

[33] C. Tzivanidis, E Bellos, G Mitsopoulos, K. A. Antonopoulos, A. Delis, (2016). Energetic and financial evaluation of a solar assisted heat pump heating system with other usual heating systems in Athens, Applied Thermal Engineering, 106, 87-97.

[34] Y. Qiu, M. Li, R. H. E. Hassanien, Y. Wang, X. Luo, Q. Yu, (2016). Performance and operation mode analysis of a heat recovery and thermal storage solar-assisted heat pump drying system, Solar Energy, 137, 225-235.

[35] T. Kim, B. Choia, Y. Hana , K. H. Do, (2018). A comparative investigation of solar-assisted heat pumps with solar thermal collectors for a hot water supply system, Energy Conversion and Management, 172, 472-484.

[36] M. Pinamonti, P. Baggio, (2020). solar-assisted heat pump systems with storage technologies for heating and cooling in residential buildings, Renewable Energy, 157, 90-99.

[37] P. Wu, Z. Wang, X. Li, Z. Xu, Y. Yang, Q. Yang, (2020). Energy-saving analysis of air source heat pump integrated with a water storage tank for heating applications, Building and Environment, 180, 107029.

[38] J. Wu, Z. Yang, Q. Wu, Y. Zhu, (2012). Transient behavior and dynamic performance of cascade heat pump water heater with thermal storage system, Applied Energy, 91, 187-196.

[39] I. Sarbu, C. Sebarchievici, (2014). General review of ground-source heat pump systems for heating and cooling of buildings, Energy and Buildings, 70, 441-454.

[40] A. Sharma, V.V. Tyagi, C.R. Chen, D. Buddhi, (2009). Review on thermal energy storage with phase change materials and applications, Renewable and Sustainable Energy Reviews, 13, 318-345.

[41] A. Hepbasli, O. Akdemir, (2004). Energy and exergy analysis of a ground source (geothermal) heat pump system, Energy Conversion and Management, 45, 737-753.

[42] H. Esen, M. Inalli, M. Esen, (2006). Technoeconomic appraisal of a ground source heat pump system for a heating season in eastern Turkey, Energy Conversion and Management, 47, 1281-1297.

[43] A. Amini, J. Miller, H. Jouhara, (2017). An investigation into the use of the heat pipe technology in thermal energy storage heat exchangers, Energy, 136, 163-172.

[44] Z. Li, Y. Lu, R. Huang, J. Chang, X. Yu, R. Jiang, X. Yu, A. P. Roskilly, (2021). Applications and technological challenges for heat recovery, storage and utilisation with latent thermal energy storage, Applied Energy, 283, 116277.

[45] M. M. Joybari, S. Seddegh, X. Wang, F. Haghighat, (2019). Experimental investigation of multiple tube heat transfer enhancement in a vertical cylindrical latent heat thermal energy storage system, Renewable Energy, 140, 234-244.

[46] S. Peng, A. Fuchs, R. A. Wirtz, (2004). Polymeric phase change composites for thermal energy storage, Applied Polymer Science, 93, 1240 –1251.

[47] D. Lefebvre, F. H. Tezel, (2017). A review of energy storage technologies with a focus on adsorption thermal energy storage processes for heating applications, Renewable and Sustainable Energy Reviews, 67, 116-125.

[48] H. Atalay, M. T. Çoban, O. Kincay, (2017). Modeling of the drying process of apple slices: Application with a solar dryer and the thermal energy storage system, Energy, 134, 382-391.

[49] H. Hasan Ismaeela , R. Yumrutaş, (2020). Investigation of a solar assisted heat pump wheat drying system with underground thermal energy storage tank, Solar Energy, 199, 538-551.

[50] E. Baniasadi, S. Ranjbar, O. Boostanipour, (2017). Experimental investigation of the performance of a mixed-mode solar dryer with thermal energy storage, Renewable Energy, 112, 143-150.

[51] G. Srinivasan, D.K. Rabha, P. Muthukumar, (2021). A review on solar dryers integrated with thermal energy storage units for drying agricultural and food products, Solar Energy, 229, 22-38.

[52] D. Jain, P. Tewari, (2015). Performance of indirect through pass natural convective solar crop dryer with phase change thermal energy storage, Renewable Energy, 80, 244-250.

[53] H. Hasan Ismaeel, R. Yumrutaş, (2019). Thermal performance of a solar-assisted heat pump drying system with thermal energy storage tank and heat recovery unit, International Journal of Energy Research, 44, 3426-3445.

[54] Taşdemiroğlu, E. Solar Energy Utilization Technical and Economic Aspe cts; Middle East Tecnical University: Ankara, Turkey, 1988.

[55] Duffie, J.A., Beckman, W.A., (1991). Solar Engineering of Thermal Process. John Willey and Sons, New York.

[56] R.Yumrutaş, O. Kaska, (2004). Experimental investigation of thermal performance of a solar assisted heat pump system with an energy storage. International Journal of Energy Research, 28, 163-175.

[57] O. Zogou, A. Stamatelos, (1998). Effect of climatic conditions on the design optimization of heat pump systems for space heating and cooling. Energy Convers. Manage, 39, 609–622.

[58] Ozisik, M.N., (1985). Heat transfer: A basic approach. McGraw-Hill, New York.

[59] R. Yumrutas, M. Unsal, (2011). Modeling and performance analysis of a house heating system with a ground coupled heat pump, Energy Science and Research, 28(2): 669-682.

[60] R. Yumrutas, M. Unsal, (2012). Energy analysis and modeling of a solar assisted house heating system with a heat pump and an underground energy storage tank, Solar Energy 86, 983-993.

APPENDIX : MATLAB Code

MATLAB is a widely used programming and numerical computing environment that offers powerful tools and features for engineers. One of the key advantages of MATLAB is its flexibility and wide range of applications. It can be used in diverse engineering fields such as mechanical, electrical, civil, chemical, and more.

MATLAB software was used to perform simulations and obtain results for extended periods. The following is the code that was utilized.

The code that was used in the system without solar collectors

```
clc
clear
close all
load('IITO','to');
rhow = 1000;    %rho water density
cpw = 4.187;    %water heat capacity
tinf = 288;     %tinf soil tempreture
fi = 0.01736;
u=1.2;
uah = 345;

%%%%carnot efficiency%%%%
% ce=0.3;
 ce=0.4;
% ce=0.5;
nohome = 1;
%%%%%%%%%%%%

%%%%tank radius%%%%
% r=2.8794;    %v100
% r=3.6278;    %v200
% r = 4.1528;    %tank radius at v=300m3
 r=4.570;     %v400
% r=4.924;     %v500
% r=5.232;     %v600
% r=5.508;     %v700
v = 4/3 * pi * r^3;

%%%%%%%%soil types%%%%%%%%
%%%%%limstone propetities
  rhos = 2500;      %rhos is soil density
  cps = 0.9;        %soil specific heat
  con = 1.3;        %soil conductivity
  alpha = 5.75e-7;  %diffusivity

%%%%%Coarse
% rhos = 2050;
% cps = 1.842;
% con = 0.519;
% alpha =1.39E-7;
```

```
%%%%%Granit
% rhos = 2640;
% cps = 0.82;
% con = 3;
% alpha =1.4E-6;
%%%%%%%%%%%%%%%%%%%%%%%%%

p= rhow * cpw / (3 * rhos *cps);
dt = 3600 * alpha / r^2;
p1=p/dt;
rt=1/(sqrt(pi*dt));
gama = 4 * pi *r* con / (nohome * uah);

sbt2=(nohome * uah) / (4 * pi * r * con * 288);
crp = [0 0 0 1 1 1 1 1 1 1 0 0];
ido = [31 31 30 31 30 31 31 28 31 30 31 30];
day=0;
ihr = zeros(1,12);
tay=zeros(10,8760);

%%%%%%%%%%%%%%%%%%%%%%%%%%%%%%%%%%%%%%%%%%%%
lg=zeros(1,12);
n=zeros(1,12);
n(1)=ido(1);
lg(1)=ido(1);
for i=2:12
    lg(i)=n(i-1)+ido(i);
    n(i)=lg(i);
end

n=182;
nn=n-182;

%%%%%%%%%%%%%%%%%%%%%%%%%%%%%%%%%%%%%%%%%%
for i = 1:12
    day = day + ido(i);
    ihr(i)= day * 24;
end
k=1;
fa = zeros(1,8760);
c1 = zeros(1,8760);
h  = zeros(1,8760);
for i = 1: 8760
    h(i) = crp(k) * sbt2*(20 - to(i));
    fa(i) = ((to(i) + 273) /288)-1;
    c1(i) = (u * (fi - fa(i)))+fi;
    if (h(i) <= 0)
        h(i) =0;
    end
    if (i == ihr(k)), k=k+1; end
end
fw= zeros(10,8760);
tdg= zeros(10,8760);
fw(1,1) = 0;
tdg(1,1) = 15; %TES water temperature at starting point
k=1;
cop=zeros(1,10);
coph=zeros(10,8760);
```

```
for m=1:10

    qly=0;  %qly is an annual dimensionless energy required of house
    wy=0;   %wy is an annual dimensionless compressor work
    qy=0;   %qy is heat input to TES tank
    tdg(m,1) = ((fw(m,1) + 1) * 288) - 273;
    wo(1) = (fi - fa(1)) * (c1(1) - fw(m,1)) / (ce* (c1(1) +1) *
gama);

    if (fw(m,1) >= c1(1)), wo(1) =0; coph(m,1)=0; end

    qn(1) = - h(1) + wo(1);
    tdg(m,2)=((fw(m,2)+1)*288)-273;
    wo(2)=(fi-fa(2))*(c1(2)-fw(m,1))/(ce*(c1(2)+1)*gama);

    if (fw(m,2)>=c1(2)),wo(2)=0;coph(m,2)=0; end
    qn(2) = - h(2) + wo(2);

    for i=3:8760
        s1=0;
        for n=1:i-2;
            s1=s1+(fw(m,n+1)-fw(m,n))/(sqrt(pi*dt*(i-n)));
        end
        wo(i)=(fi-fa(i))*(c1(i)-fw(m,i-1))/(ce*(c1(i)+1)*gama);

        if (fw(m,i-1)>=c1(i)),wo(i)=0;coph(m,i)=0; end

        qn(i) = - h(i) + wo(i);
        tdg(m,i)=((fw(m,i)+1)*288)-273;

        wy=wy+wo(i)*dt;
        qly=qly+h(i)*dt;
        qy=qy+qn(i)*dt;
        if (i~=ihr(k)), continue; end

        tay(m,k)=tdg(m,i);
        k=k+1;
        if (i==8760),fw(1,1)=fw(m,8760); end
    end
    if (m~=1)
        qst=p*(fw(m,8760)-fw(m,1));
    else
        qst=p*(fw(m,8760)-0);
    end

    cop(m)=qly/wy;
    k=1;
end
```

The code that was used in the system with solar collectors

```
clc
clear
close all
%load('toit','ii','to');
load('IITO','ii','to');
%(to & ii) are external data to be imported
rhow = 1000;    %rho water density
cpw = 4.187;     %water heat capacity
tinf = 288;     %273 + 15 , tinf = 15 c, tinf soil tempreture
fi = 0.01736;   %fi = (293 - 288) / 288 = 0.01736
u=1.2;
uah = 345;
uahe = uah / u;
 ac = 20;        %collector area
% ac=25;
% ac=30;
% ce=0.3;
ce = 0.4;       %carnot efficiency
% ce=0.5;
nohome = 1;
%%%%%%%%%%%%
% r=2.8794;    %v100
% r=3.6278;    %v200
% r = 4.1528;    %tank radius at v=300m3
 r=4.570;     %v400
% r=4.924;     %v500
% r=5.232;     %v600
% r=5.508;     %v700
v = 4/3 * pi * r^3;


%%%%%%%%soil types%%%%%%%%
%limstone propetities
% rhos = 2500;      %rhos is soil density
% cps = 0.9;        %soil specific heat
% con = 1.3;        %soil conductivity
% alpha = 5.75e-7;  %diffusivity
%%%%%%Coarse
% rhos = 2050;
 %cps = 1.842;
 %con = 0.519;
 %alpha =1.39E-7;
%%%%%%Granit
  rhos = 2640;
  cps = 0.82;
  con = 3;
  alpha =1.4E-6;
%%%%%%%%%%%%%%%%%%%%%%%%%
fr=0.9;
taln=0.8;
tgalf=taln;
ul=8;    %ul or UL its  overall loss coefficient of the collector
p= rhow * cpw / (3 * rhos *cps);
dt = 3600 * alpha / r^2;
p1=p/dt;
rt=1/(sqrt(pi*dt));
gama = 4 * pi *r* con / (nohome * uah);
sbt1=(nohome * ac) / (4 * pi * r * con * 288);
sbt2=(nohome * uah) / (4 * pi * r * con * 288);
```

```
crp = [0 0 0 1 1 1 1 1 1 1 0 0];
ido = [31 31 30 31 30 31 31 28 31 30 31 30];
ef=[0.56 0.55 0.49 0.39 0.32 0.27 0.29 0.35 0.40 0.47 0.5 0.55];
re=[0.1 0.1 0.1 0.1 0.1 0.1 0.3 0.7 0.5 0.3 0.1 0.1]; %re is monthly
average reflectivity of earth
day=0;
ihr = zeros(1,12);
tay=zeros(10,8760);
%%%%%%%%%%%%%%%%%%%%%%%%%%%%%%%%%%%%%%%%%%%%
lg=zeros(1,12);
del=zeros(1,365);
n=zeros(1,12);
n(1)=ido(1);
lg(1)=ido(1);
for i=2:12
    lg(i)=n(i-1)+ido(i);
    n(i)=lg(i);
end
cr1=2*pi/365;
cr2=pi/180;
 pir = zeros(1,365);
 delta=zeros(1,365);
for i=1:365
    pir(i)=cr1*(284+i);
    delta(i)=23.45*sin(pir(i));
    del(i)=cr2*delta(i);
end
bt=37.1;
fai=37;
fii=fai*pi/180;
btt=bt*pi/180;
j1=1;
dec=2;
ihd=0;
itd=0;
ihm=0;
itm=0;
ihy=0;
ity=0;
n=182;
t=0;
tem=0;
tsum=0;
gs=1353;
kt= zeros(1,8760);
iio=zeros(1,8760);
idi=zeros(1,8760);
rb=zeros(1,8760);
it=zeros(1,8760);
iih=zeros(1,8760);
itdav=zeros(1,365);
ihdav=zeros(1,365);
ihmav=zeros(1,12);
itmav=zeros(1,12);
tam=zeros(1,12);
tal=zeros(1,8760);
w=zeros(1,8760);
w1=zeros(1,8760);
w2=zeros(1,8760);
nn=n-182;
for i=1:8760
```

```
    if (n==365),n=0; end
        n=n+1;
        if (nn==365),nn=0; end
        nn=nn+1;
        l=floor(((i-1)/24)+1);     %floor is used to make L integer
number
        w1(i)=15*(t-12)*pi/180;
        w2(i)=15*(t-11)*pi/180;
        w(i)=(w1(i)+w2(i))/2;
        rin(nn)=2*pi*n/365;

rq(nn)=(43200.*(gs./pi)).*(1+(0.033.*cos(rin(nn)))).*(cos(fii).*cos(
del(n)).*(sin(w2(i))-sin(w1(i)))+((w2(i)-
w1(i)).*sin(fii).*sin(del(n)))); %iq represent I_0 in the equations
        iio(i)=abs(rq(nn));

        kt(i)=ii(i)/iio(i)*41870;

    if (kt(i)<=0.35)
        idi(i)=1-0.249*kt(i);
    elseif (kt(i)<=0.75)
        idi(i)=1.557-1.84*kt(i);
    else
        idi(i)=0.177;
    end
    rbc(i)=((cos(fii-btt)*cos(del(n))*cos(w1(i)))+(sin(fii-
btt)*sin(del(n))))/((cos(fii)*cos(del(n))*cos(w1(i)))+(sin(fii)*sin(
del(n))));  % to calculate Rb
    bs(i)=abs(rbc(i));
    if(bs(i)>=2)
        rb(i)=0.4;
    else
        rb(i)=bs(i);
    end
    ar1(i)=(1-idi(i))*rb(i);
    ar2(i)=idi(i)*((1+cos(btt))/2);
    ar3(i)=re(j1)*((1-cos(btt))/2);
    rcf(i)=ar1(i)+ar2(i)+ar3(i);
    it(i)=rcf(i)*ii(i)*41870/3600;  %% where rcf (represent R in the
article) is the ratio of total radiation on the tilted surface to that
on a horizontal surface.
    iih(i)=ii(i)*41870/3600;        % This (iih(i)) is to transfer ii
unit to w/m2 to unity with it for comparison between them only
    %%%%%%%%%%%%%%%%%%%%%%%%%%%%%%%%
    tetaz=acos(sin(fii)*sin(del(n))+cos(fii)*cos(del(n))*cos(w(i)));
    tq=abs(rb(i)*cos(tetaz));
    if (tq>1)
        tal(i)=taln;
    else
       teta=acos(tq);
    end
    if (dec==1)
       bo=-0.10;
    else
       bo=-0.17;
    end
        amod=1+bo*(1/cos(teta)-1);
    if (amod<=0.2)
       amod=0.9-0.01*teta*180/pi;
   end
    if (amod>=1), tal(i)=taln;
```

```
    else
       tal(i)=taln*amod;
    end
    %%%%%%%%%%%%%%%%%%%%%%%%%%%%%%%%
    k1=floor(i/24);
    k2=24*k1;
    if (i==k2),t=-1;end
    t=t+1;
    ihd=ihd+ii(i);
    itd=itd+it(i);
    tem=tem+to(i);
    m1=i/24;
    m2=24*m1;
    if (i~=m2), continue; end
    ihdav(l)=ihd/24*41870/3600;
    itdav(l)=itd/24;
    ihm=ihm+ihd;
    itm=itm+itd;
    ihd=0;
    itd=0;
    km=lg(j1)*24;
    kl=ido(j1)*24;
    if (i~=km), continue; end
    ihmav(j1)=ihm/kl*41870/3600;
    itmav(j1)=itm/kl;
    tam(j1)=tem/kl;
    ihy=ihy+ihm;
    ity=ity+itm;
    tsum=tsum+tam(j1);
    tdif=20-tam(j1);
    j1=j1+1;
    ihm=0;
    itm=0;
    tem=0;
end
ihory=ihy*41870/(8760*3600);
itily=ity/8760;

% save('result','fw');
%%%%%%%%%%%%%%%%%%%%%%%%%%%%%%%%%%%%%%%%%%
for i = 1:12
    day = day + ido(i);
    ihr(i)= day * 24;
end
k=1;
fa = zeros(1,8760);
c1 = zeros(1,8760);
h = zeros(1,8760);
for i = 1: 8760
    h(i) = crp(k) * sbt2*(20 - to(i));
    fa(i) = ((to(i) + 273) /288)-1;
    c1(i) = (u * (fi - fa(i)))+fi;
    if (h(i) <= 0)
        h(i) =0;
    end
    if (i == ihr(k)), k=k+1; end
end
fw= zeros(10,8760);
tdg= zeros(10,8760);
del=zeros(365);
fw(1,1) = 0;
```

```
tdg(1,1) = 15; %TES water temperature at start point
v = 4/3 * pi * r^3;
k=1;
cop=zeros(1,10);
r1=zeros(1,10);
r2=zeros(1,10);
r3=zeros(1,10);
r4=zeros(1,10);
r5=zeros(1,10);
qls = zeros(1,8760);
e =zeros(1,8760);
coph=zeros(10,8760);

for m=1:10
    efc=0;  %efc is efficiency of a flat plate solar collector
    qsy=0;  %qsy is an annual dimensionless solar heat gain
    qly=0;  %qly is an annual dimensionless energy required of house
    wy=0;   %wy is an annual dimensionless compressor work
    qy=0;   %qy is heat input to TES tank
    tdg(m,1) = ((fw(m,1) + 1) * 288) - 273;
    wo(1) = (fi - fa(1)) * (c1(1) - fw(m,1)) / (ce* (c1(1) +1) *
gama);

    if (fw(m,1) >= c1(1)), wo(1) =0 ; coph(m,1)=0 ; end
    if ( it(1) <= 0)
        e(1)=0;
    else
        qls = (tdg(m,1) - to(1)) / it(1);
        if(qls >= 0.72)
            e(1) = 0;
        else
            e(1) = 0.72 - 6.4 * qls;
            if(e(1) <= 0 )
                e(1) = 0;
            elseif (e(1) > 0.72 )
                e(1) = 0.72;
            end
        end
    end
    s(1) = sbt1 * e(1) * it(1); % sbt1 is Q in eqn.6, q
    qn(1) = s(1) - h(1) + wo(1);
    tdg(m,2)=((fw(m,2)+1)*288)-273;
    wo(2)=(fi-fa(2))*(c1(2)-fw(m,1))/(ce*(c1(2)+1)*gama);

    if (fw(m,2)>=c1(2)),wo(2)=0; coph(m,2)=0; end
    if(it(2)<=0)
        e(2)=0;
    else qls = (tdg(m,1) - to(2)) / it(2);
        if(qls >= 0.72)
            e(2) = 0;
        else
            e(2) = 0.72 - 6.4 * qls;
            if(e(2) <= 0 )
                e(2) = 0;
            elseif (e(2) > 0.72)
                e(2) = 0.72;
            end
        end
    end
    s(2) = sbt1 * e(2) * it(2);
    qn(2) = s(2) - h(2) + wo(2);
```

```
    for i=3:8760
        s1=0;
        for n=1:i-2;
            s1=s1+(fw(m,n+1)-fw(m,n))/(sqrt(pi*dt*(i-n)));
        end
        wo(i)=(fi-fa(i))*(c1(i)-fw(m,i-1))/(ce*(c1(i)+1)*gama);

        if (fw(m,i-1)>=c1(i)),wo(i)=0; coph(m,i)=0; end
        if(it(i)<=0)
            e(i)=0;
        else
            qls = (tdg(m,i-1) - to(i)) / it(i);
            if(qls > 0.72)
                e(i) = 0;
            else     e(i) = 0.72 - (6.4 * qls);
                if(e(i) <= 0 )
                    e(i) = 0;
                elseif (e(i) > 0.72)
                    e(i) = 0.72;
                end
            end
        end
        s(i) = sbt1 * e(i) * it(i);
        qn(i) = s(i) - h(i) + wo(i);
        tdg(m,i)=((fw(m,i)+1)*288)-273;   %tdg(m,i)=hourly TES water
temperature for 10 years in C
        qsy=qsy+s(i)*dt;
        wy=wy+wo(i)*dt;
        qly=qly+h(i)*dt;
        qy=qy+qn(i)*dt;
        if (i~=ihr(k)), continue; end
        efc=efc/(ido(k)*24);
        tay(m,k)=tdg(m,i);
        k=k+1;
        if (i==8760),fw(1,1)=fw(m,8760); end
    end
    if (m~=1)
        qst=p*(fw(m,8760)-fw(m,1));
    else
        qst=p*(fw(m,8760)-0);
    end
        qt=qsy+wy;
        r1(m)=qsy*100/qt;   % r1 yearly (solar fraction) charged to
the system
        r2(m)=wy*100/qt;   % r2 yearly heat pump (work fraction)
        r3(m)=qst*100/qt;  % r3 yearly (stored energy) fraction
        r4(m)=qly*100/qt;  % r4 yearly house heat (load fraction)
        r5(m)=(qy-qst)*100/qt;  %r5 yearly heat (lost fraction)
charged to the system,
    cop(m)=qly/wy;
    k=1;
end
```

CURRICULUM VITAE

PERSONAL DETAILS

Name SURNAME: Ghadir CHAHID

EDUCATION

Septemper 2019 – July 2023 **Gaziantep University, Gaziantep, Turkey**
Master's Degree in Mechanical Engineering – Energy Division

September 2000 - June 2006 **University of Aleppo, Aleppo, Syria**
Bachelor's Degree in Energy Engineering

September 1997 - June 2000 **Rabaa Al Adawiya High School, Doha, Qatar**
High School Diploma

EXPERIENCE:

- Aleppo Thermal Station, June 2005 - July 2005 (During Fourth Year of University Education).
    - Participated in a pre-graduating boot camp at Aleppo Thermal Station before graduating from university.
    - Attended daily sessions during the fourth year of university education, enhancing knowledge and skills in Steam turbines, cooling towers and boilers operation.
- Technical Office, General Establishment of Syrian Railways, Aleppo, Syria, August 2007 - October 2013.
- Shareholder of Urban Research Centre; a company specialized in urban planning, new energy studies and implementation of engineering projects in Syria, 2016 to present.